INDIAN INSTITUTE OF SCIENCE

DEPARTMENT OF INSTRUMENTATION AND APPLIED PHYSICS

IN252 - OPTICS: MATERIALS AND DEVICES

Assignment 4

Chaitali Shah
(SR No: 01-02-04-10-51-21-1-19786)

Date: November 29, 2023

Measurement of Band Gap of Selenium using absorption data in Ultraviolet-visible region.

Photons get absorbed in a material when their energy exceeds its bandgap. Therefore, one can determine the bandgap by measuring the absorption spectrum of a material. J. Tauc used the absorption data of amorphous Si and Ge to determine their bandgap.

The Ultraviolet-visible region spectrophotometer reflectivity and transmittivity data for Selenium has been given.

1. Plot the Reflectivity and Transmittivity against wavelength.

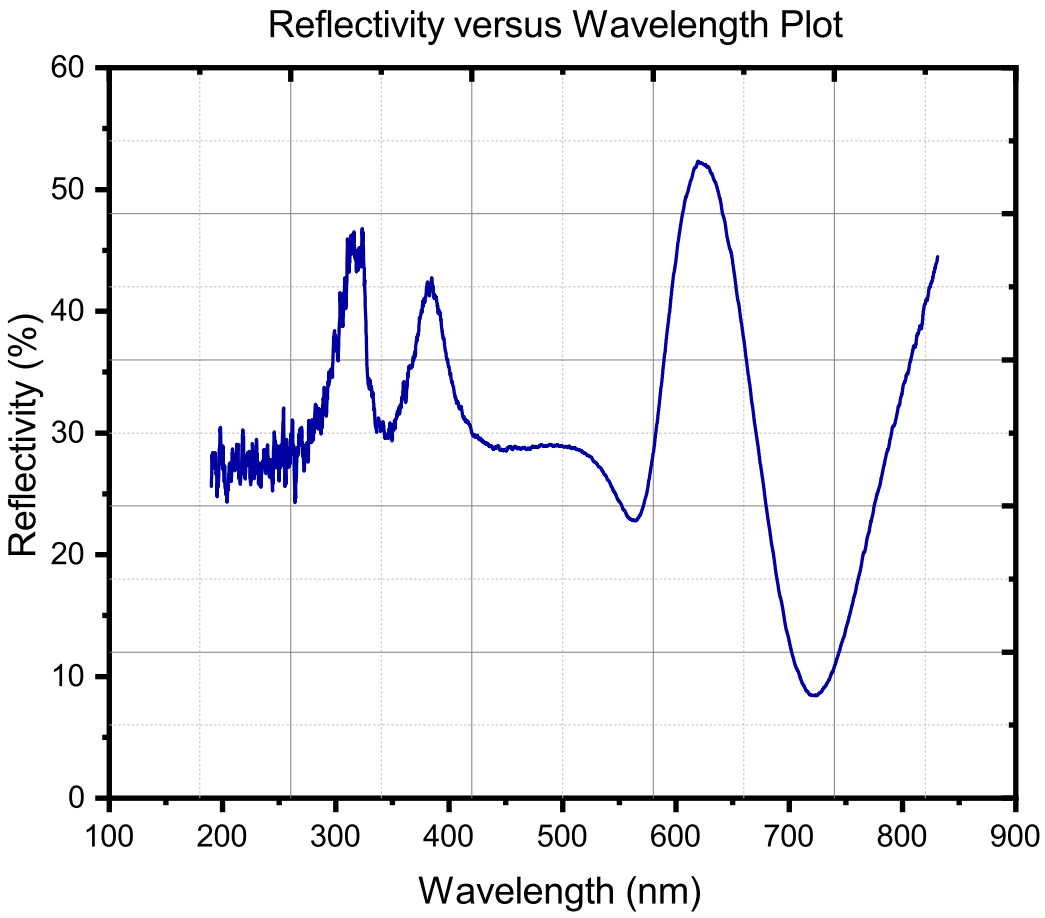

Figure 1: The plot of Reflectivity R against wavelength λ

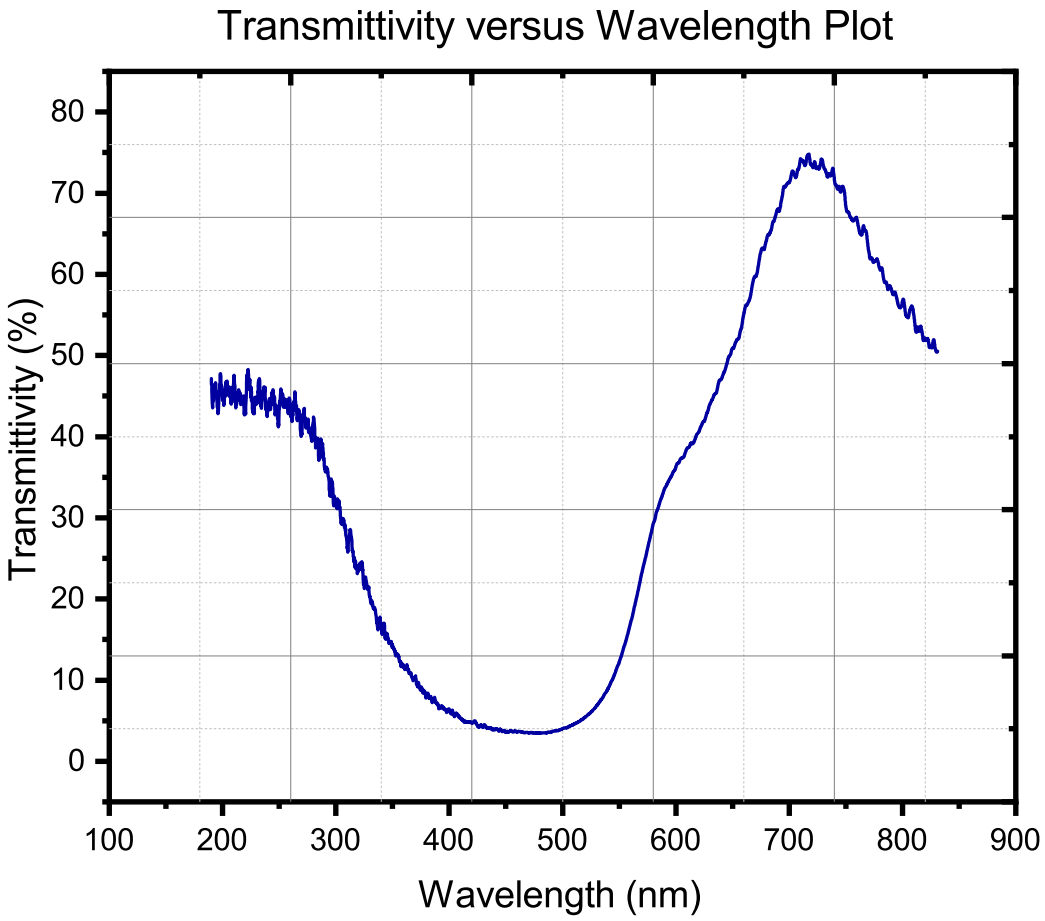

Figure 2: The plot of Transmittivity T against wavelength λ

2. Plot the Absorptivity versus wavelength.

   The absorptivity is found by using the following relation.

$$A(\%) = 100 - T(\%) - R(\%)$$

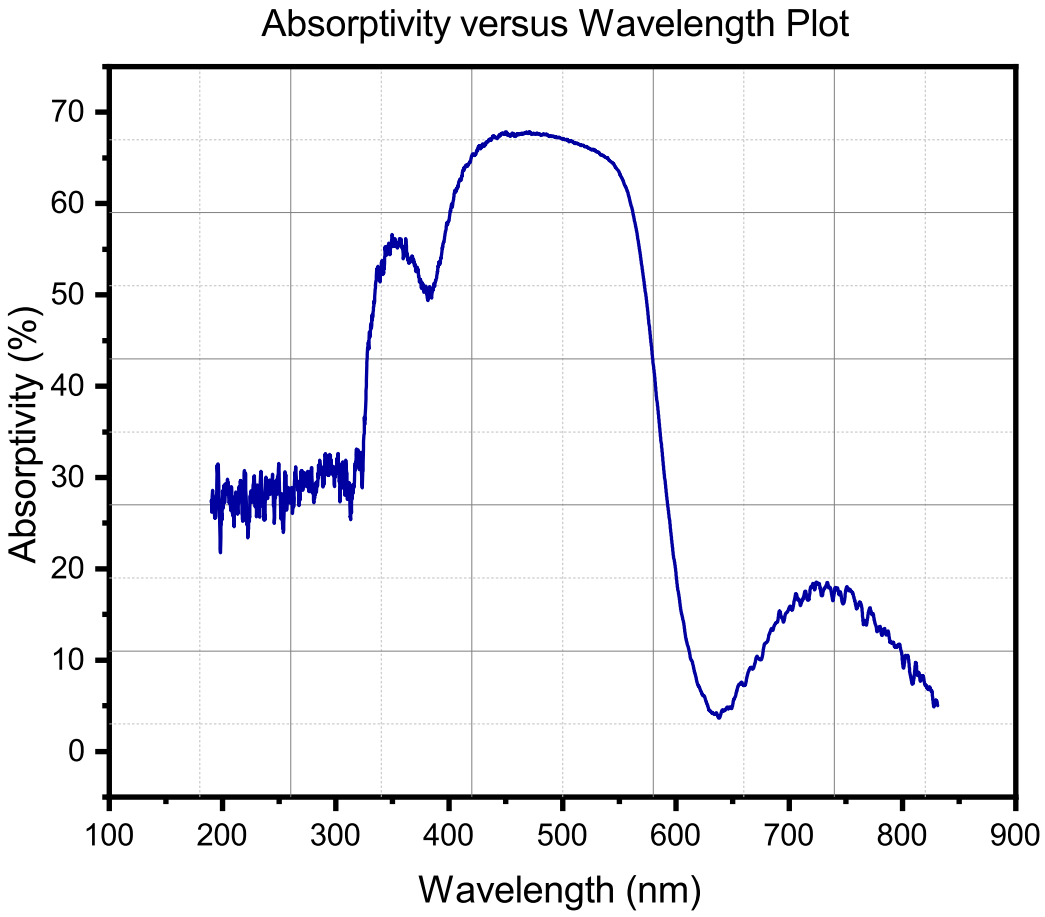

Figure 3: The plot of Absorptivity A against wavelength λ

3. Considering whether Se is direct or indirect band gap material, do the Tauc plot.

   Selenium is a Direct Band Gap material.

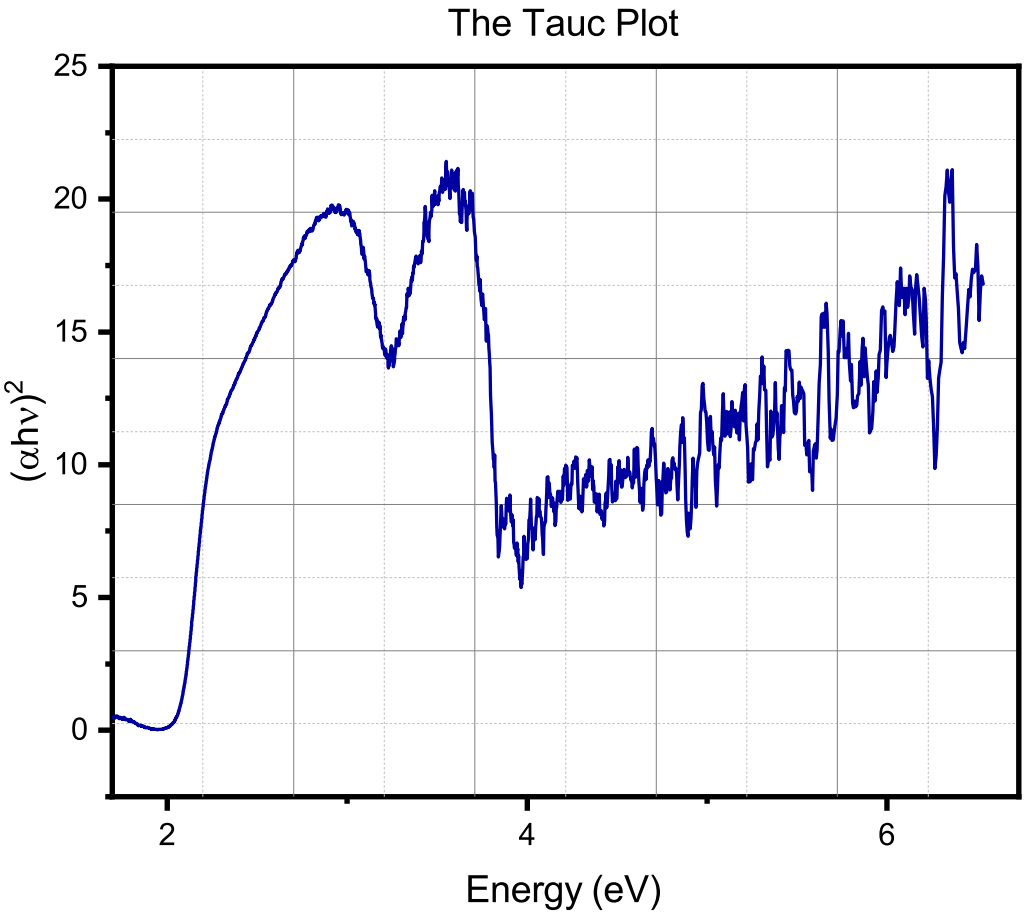

Figure 4: The plot of $(\alpha h\nu)^2$ against energy, $h\nu$

References

(a) J. Tauc, Optical properties and electronic structure of amorphous Ge and Si, Materials Research Bulletin,Volume 3, Issue 1, 1968, Pages 37-46, ISSN 0025-5408

(b) Habubi, Nadir Bakr, Nabeel Salman, Sabah. (2013). Optical parameters of amorphous selenium deposited by thermal evaporation technique. Physical Chemistry: An Indian Journal. 8. 54-58.

4. Use the Tauc plot to determine the bandgap.

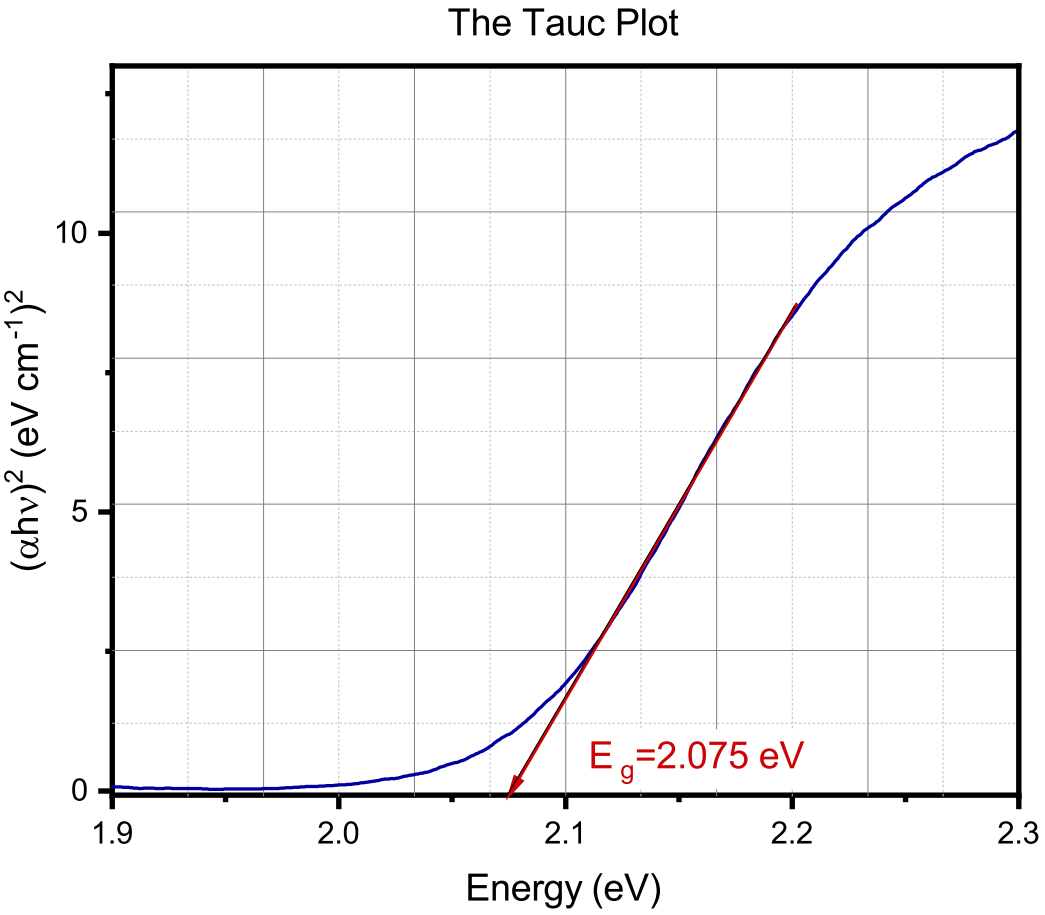

Figure 5: Magnified plot of $(\alpha h\nu)^2$ against energy, $h\nu$ with extrapolation to find band gap E_g

The extrapolation of the linear portion of the plot on to the energy axis determines the energy band gap.
From the Tauc plot the bandgap is found to be $E_g = 2.075$ eV.

5. In the absorptivity plot you may notice a small peak between the wavelengths 650nm to 800nm. What do you think is its source?

   There could be many sources of such peaks.

   (a) The defects in the amorphous selenium material lead to lack of homogeneity in the band gap that may lead to transitions for photon energies less that the band gap. Amorphous materials lack long range orders and hence their spectra can have peaks at many energy levels.

   (b) The peak can be majorly attributed to the non-radiative transitions between their valence and conduction bands. Phonon assisted non-radiative transistions require lower energy that the band gap and contribute to peaks at higher wavelengths.

INDIAN INSTITUTE OF SCIENCE

DEPARTMENT OF INSTRUMENTATION AND APPLIED PHYSICS

IN252 - OPTICS: MATERIALS AND DEVICES

Assignment 5

Chaitali Shah
(SR No: 01-02-04-10-51-21-1-19786)

Date: November 29, 2023

Distributed Bragg Reflectors

Distributed Bragg Reflectors consisting of alternate layers of dielectric materials with different refractive index are considered.

1. Explain the origin of the high reflectivity of such periodic structure. What is the optimum thickness required to have a high reflectivity?

The high reflectivity results from constructive interference of light reflecting on multiple interfaces. For constructive interference, the reflected waves should be in phase with each other. For every layer the light propagates into the stack, it must travel back twice the path to reach the surface on reflection.

This can be achieved by using layers of thickness that correspond to a quarter of the wavelength $\frac{\lambda}{4n}$. This leads to constructive interference because the wave travels a distance of $\frac{\lambda}{2n}$ per layer which results in a phase shift of $\frac{\lambda}{2n} \times 2\pi n = \pi$ per layer. The total phase shift is π for an odd number of layers and there is not phase shift for an even number of layers. If the top layer has the higher index, then after travelling an odd number of layers, the reflection will at a high-to-low interface, so no phase shift will occur resulting in an overall phase shift of π. For an even number of layers, the wave reflects at a low-to-high interface, causing a phase shift of π, combined with no phase shift for travelling through an even number of layers resulting in a overall phase shift of π at the surface. The condition is met even in case of multiple reflections within the DBR.

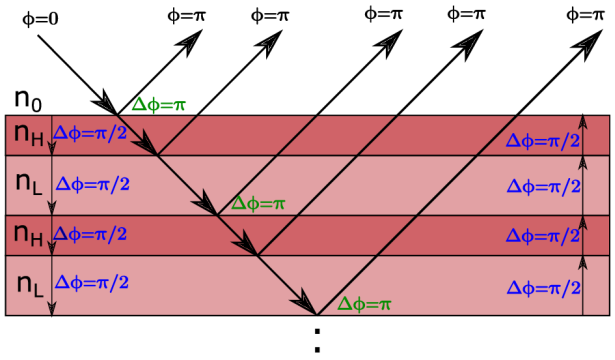

Figure 1: Distributed Bragg Reflector
Reprinted from Deposition and Characterization of Dielectric Distributed Bragg Reflectors, M. Lapp

The optimum thickness of the two layers to get a high reflectivity is given by,

$$d_1 = \frac{\lambda}{4n_1} \quad d_2 = \frac{\lambda}{4n_2}$$

The periodicity of the structure is given by,

$$D = d_1 + d_2 = \frac{\lambda}{4}\left(\frac{1}{n_1} + \frac{1}{n_2}\right)$$

2. We consider two alternate dielectric material shaving refractive index 1.24 and 2.08 respectively. Design in Lumerical an efficient Brag mirror to obtain a near unity reflection at around 600 nm.Plot reflectivity versus number of layers. Deduce the optimum number of layers required for near unity reflection.

$$d_1 = \frac{600\text{nm}}{4 \times 1.24} = 120.96\text{nm}, \quad d_2 = \frac{600nm}{4 \times 2.08} = 72.12\text{nm}$$

The reflectivity spectrums for different number of bilayers are shown in the following plot.

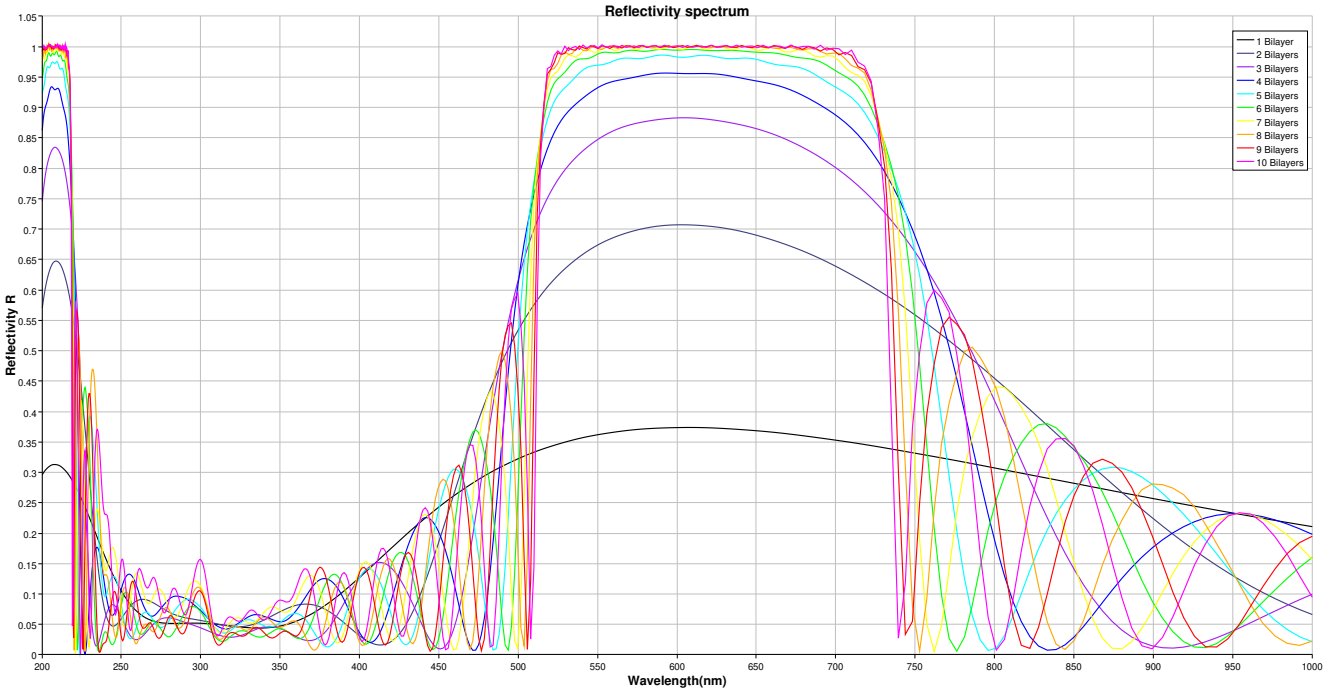

Figure 2: The plot of Reflectivity R against wavelength λ for different number of Bilayers

It can be seen that the reflectivity at 600 nm increases with increasing number of bilayers. Also the plot becomes sharper and starts resembling a rectangular function as the number of bilayers increases. The ripples increase and grow sharper for large number of bilayers. The finiteness of number of layers leads to the formation of side lobes.

Theoretically, the reflectivity as a function of the number of bilayers is given by,

$$R = \left[\frac{n_o(n_2)^{2N} - n_s(n_1)^{2N}}{n_o(n_2)^{2N} + n_s(n_1)^{2N}} \right]^2$$

Here, Refractive index of medium, $n_o = 1$,
Refractive index of substrate, $n_s = 1.5$,
Refractive index of material in first layer, $n_1 = 1.24$,
Refractive index of material in second layer, $n_2 = 2.08$
and N is the number of bilayers.

Therefore,

$$R = \left[\frac{(2.08)^{2N} - 1.5(1.24)^{2N}}{(2.08)^{2N} + 1.5(1.24)^{2N}}\right]^2$$

The plot of reflectivity at 600 nm, both as predicted by the formula and as observed in the simulation, versus the number of bilayers is shown below.

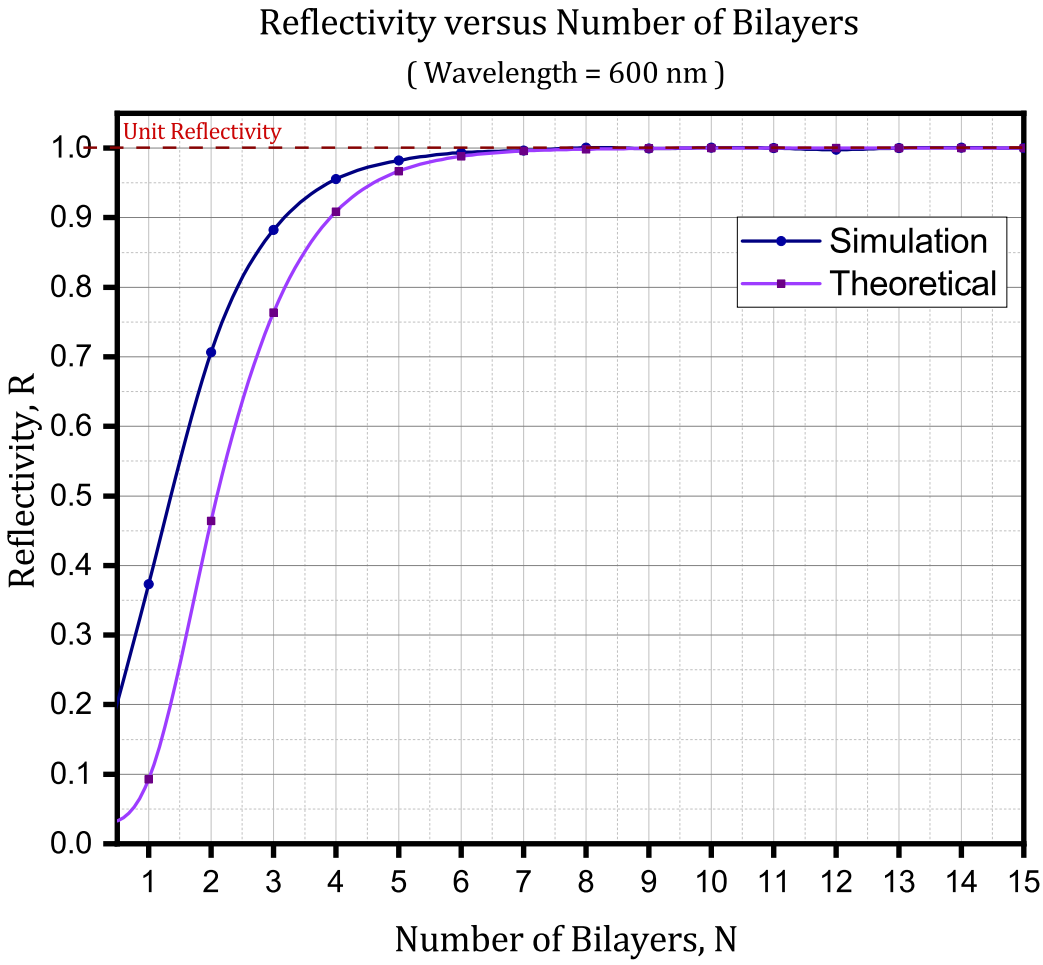

Figure 3: The plot of Reflectivity R (simulated and theoretical) versus the number of bilayers N

It can be seen in Fig. 3 that the reflectivity closely approaches unity 8 bilayer onwards, in both simulated and estimated results. So 8 would be the minimum number of bilayers required for unit reflectivity in this case. The performance improves with increase in the number of bilayers.

3. Comment on the bandwidth of the DBR. How can you increase the FWHM in such devices?

Theoretically, the frequency bandwidth of the DBR is given by

$$\Delta f = f_0\left(\frac{4}{\pi}\right)sin^{-1}\left(\frac{n_2 - n_1}{n_2 + n_1}\right)$$

where,

$$f_0 = \frac{c}{\lambda_0} = \frac{3\times10^8 m/s}{600\times10^{-9}m} = 5\times10^{14}Hz = 500 \text{ THz}$$

$$\Delta f = 500\left(\frac{4}{\pi}\right)sin^{-1}\left(\frac{2.08 - 1.24}{2.08 + 1.24}\right) \text{ THz} = 162.84 \text{ THz}$$

We can find the bandwidth in terms of wavelength as follows.

$$\Delta\lambda = \frac{\lambda_0^2}{c}\Delta f = 195.41 \text{ nm}$$

As, seen from the Fig. 2, the results found by simulation are close to the theoretical predictions.

The Full Width Half Maxima (FWHM) depends on the number of bilayers as seen in Fig. 2. FWHM decreases with increase in the number of bilayers. It can also be change by changing the materials. FWHM increases as the difference between the refractive indices of the two materials is increased.

INDIAN INSTITUTE OF SCIENCE

DEPARTMENT OF INSTRUMENTATION AND APPLIED PHYSICS

IN252 - OPTICS: MATERIALS AND DEVICES

Assignment 6

Chaitali Shah
(SR No: 01-02-04-10-51-21-1-19786)

Date: November 29, 2023

Synthesis of Gold Nanoparticle Solution

1 Introduction

Gold nanoparticles (Au NPs) can be synthesized in aqueous solution by reduction of a gold salt. The solution of the gold salt is heated and rapidly stirred while a reducing agent is added. This causes the gold ions to be reduced to neutral gold atoms. As more and more of these gold atoms form, the solution becomes supersaturated, and gold gradually starts to precipitate in the form of sub-nanometer particles (nucleation). The rest of the gold atoms that form stick to the existing particles (growth), and, if the solution is stirred vigorously enough, the particles will be fairly uniform in size.

The method pioneered by J. Turkevich et al. in 1951 is the simplest one available. Generally, it is used to produce modestly monodisperse spherical gold nanoparticles suspended in water of around 15 nm in diameter. It involves the reaction of small amounts of hot chlorauric acid ($H[AuCl_4]$) with small amounts of sodium citrate solution. The gold nanoparticles are formed because the citrate ions act as both a reducing agent, and a capping agent.

2 Experiment

2.1 Materials

Round bottom flask, caps, condenser, hotplate-oil bath-thermometer, egg magnetic bar

2.2 Chemicals

Trisodium citrate ($Na_3C_6H_5O_7.2H_2O$), Chloroauric acid ($H[AuCl_4]$), sodium salt ($NaCl$).
Use only ultra-pure water (milli-Q) for all solutions and rinsing.

2.3 Instrument

Absorbance spectrometer.

2.3.1 Synthesis of Au NPs by the Turkevich method

- The given chloroauric acid solution in water has a concentration of c = 4.1 g/L. Calculate the volume needed to get 6 mg of Au nanoparticles.
  The molar mass of gold Au is 196.9665, chlorine is 35.453 g and hydrogen H is 1.007 g.
  The molar mass of cholorauric acid $H[AuCl_4]$ is 339.786 g.
  339.786 g of $H[AuCl_4]$ has 196.9665 g of Au.
  $\therefore$ Mass of $H[AuCl_4]$ for 6 mg of Au nanoparticles $= 6 \times 10^{-3} \times \left(\frac{339.786}{196.9665}\right) = 10.350$ mg.
  Volume of chloroauric acid solution required $= \frac{10.350 \times 10^{-3}}{4.1}$
  Volume of chloroauric acid solution required $= 2.5245$ mL.

- Prepare 5 mL of a solution of trisodium citrate in water with c = 11g/L.
- Set the three-neck round bottom flask up with the condenser in the oil bath on the hotplate.
- Put 92.5mL of water in the three-neck round bottom flask and add the calculated volume of the chloroauric acid solution under stirring.
- Heating up the flask to $90°C$.
- After the temperature is stabilized at $90°C$, inject the 5 mL of the prepared citrate solution.
- Leave 20 minutes under stirring.
- Stop the heating and leave the flask exposed to air until it cools down to ambient temperature (keep stirring).

2.3.2 Study of the colloidal stability

- Prepare 5 mL of two solutions of NaCl in water with c1 = 1.5 g/L and c2 = 0.15 g/L.
- Prepare three vials with 0.5 mL of the Au NPs solution and 2 mL of water/
- In each vial add respectively 100 L of water, of NaCl solution at c1 and c2.
- Stir manually the vials.

2.3.3 UV-visible absorption measurements

- Put the solution in the UV plastic cuvettes
- Measure the absorbance spectra of three different samples from 200 to 800 nm.
- Measure the absorbance spectra of the given silver NPs solutions with same parameters.

3 Discussion of the results

a. Write down the reduction equation involved in the synthesis of the Au nanoparticles.

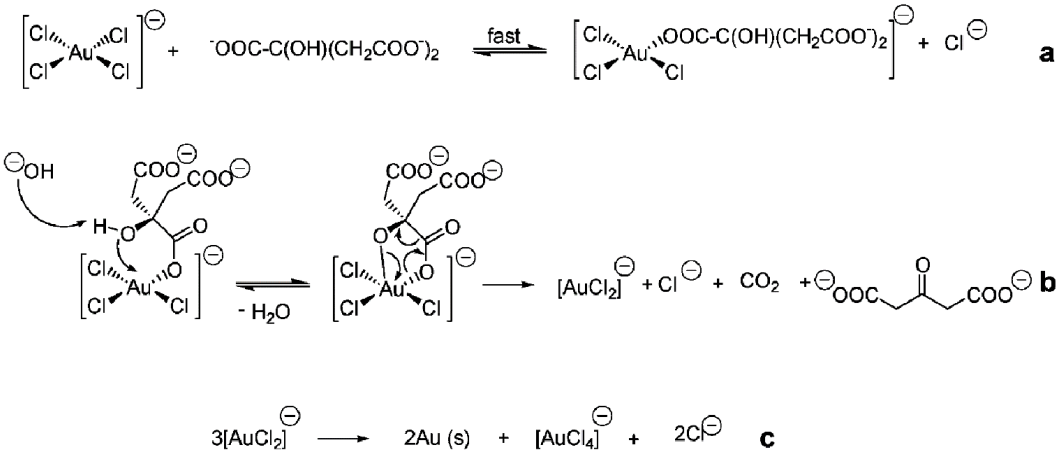

Figure 1: The mechanism of gold reduction: (a) Ligand exchange reaction (b) decarboxylation and reduction of Au(III) species and (c) disproportionation of aurous species and the subsequent formation of Au (O) atoms

The reduction equation can be written as:

$$2[AuCl_4]^- + 3(C_6H_5O_7)^{-3} \rightarrow 2Au + 3CO_2 + 3C_5H_4O_5^{-2} + 3H^+ + 8Cl^-$$

b. Do a schematic representation of the nanoparticles.

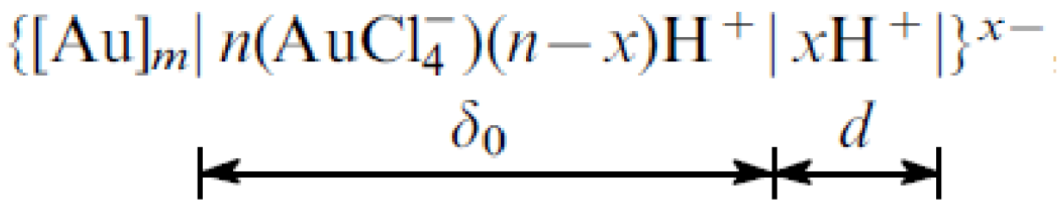

Figure 2: Chemical scheme of nanoparticle colloidal system

In Fig. 3, $[Au]_m$ is the metal core, where m is the number of atoms it consists of, n is the number of adsorbed ions $AuCl_4^-$ (n i m), δ_0 is the thickness of adsorption layer and is the diffuse layer thickness.

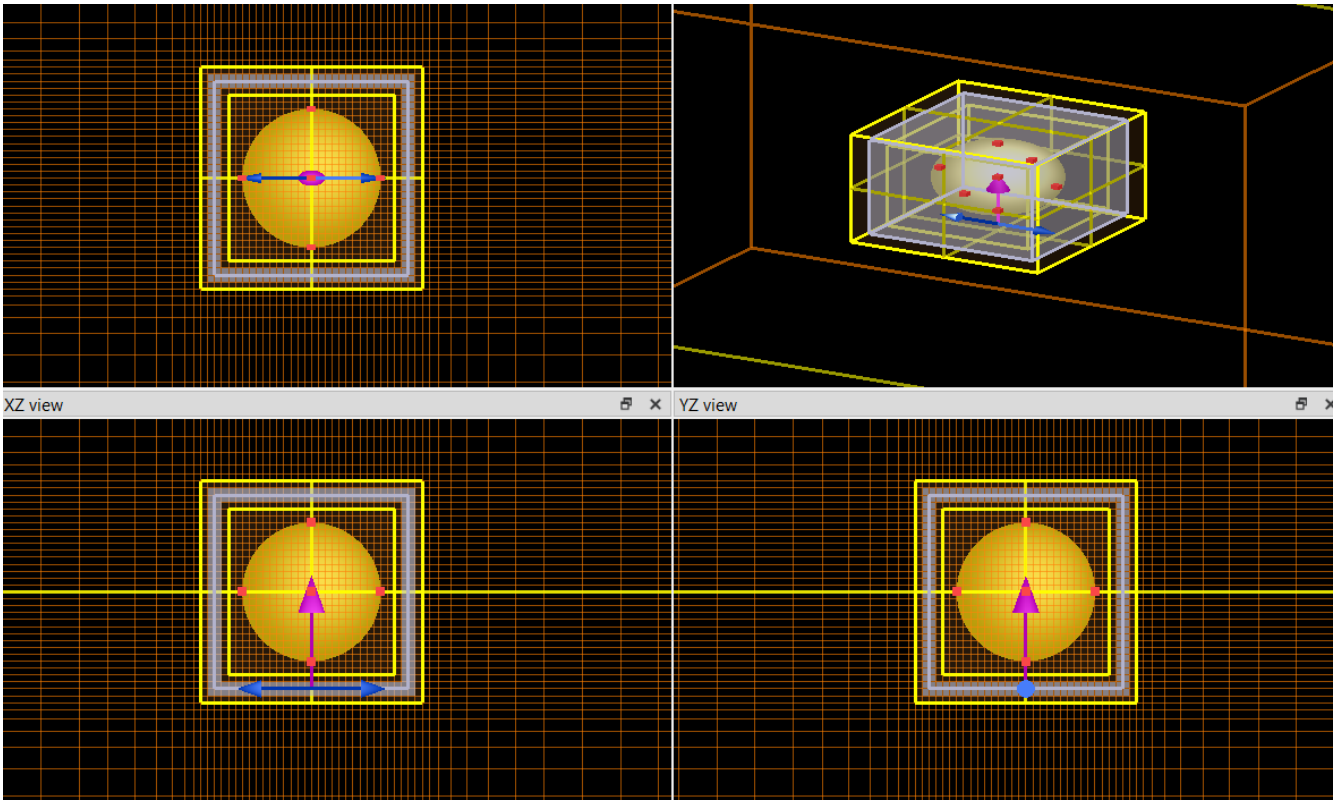

Figure 3: Schematic Representation in Lumerical

c. How can you explain their stability in solution?
Stabilizers are used to preserve the properties of solutions of colloids. They are substances that prevent the spontaneous coagulation of the particles. Here, the citrate anion ($Na_3C_6H_5O_7.2H_2O^{-3}$) acts as both a reducing agent and stabilizer.

d. Explain the UV-visible spectra of the Au Nanoparticles solution and compare it with the Ag Nanoparticles one. Simulate using Lumerical how does the extinction spectra changes as a function of particle radius (5-50 nm).

The UV-visible spectra of Gold Nanoparticles is shown below.

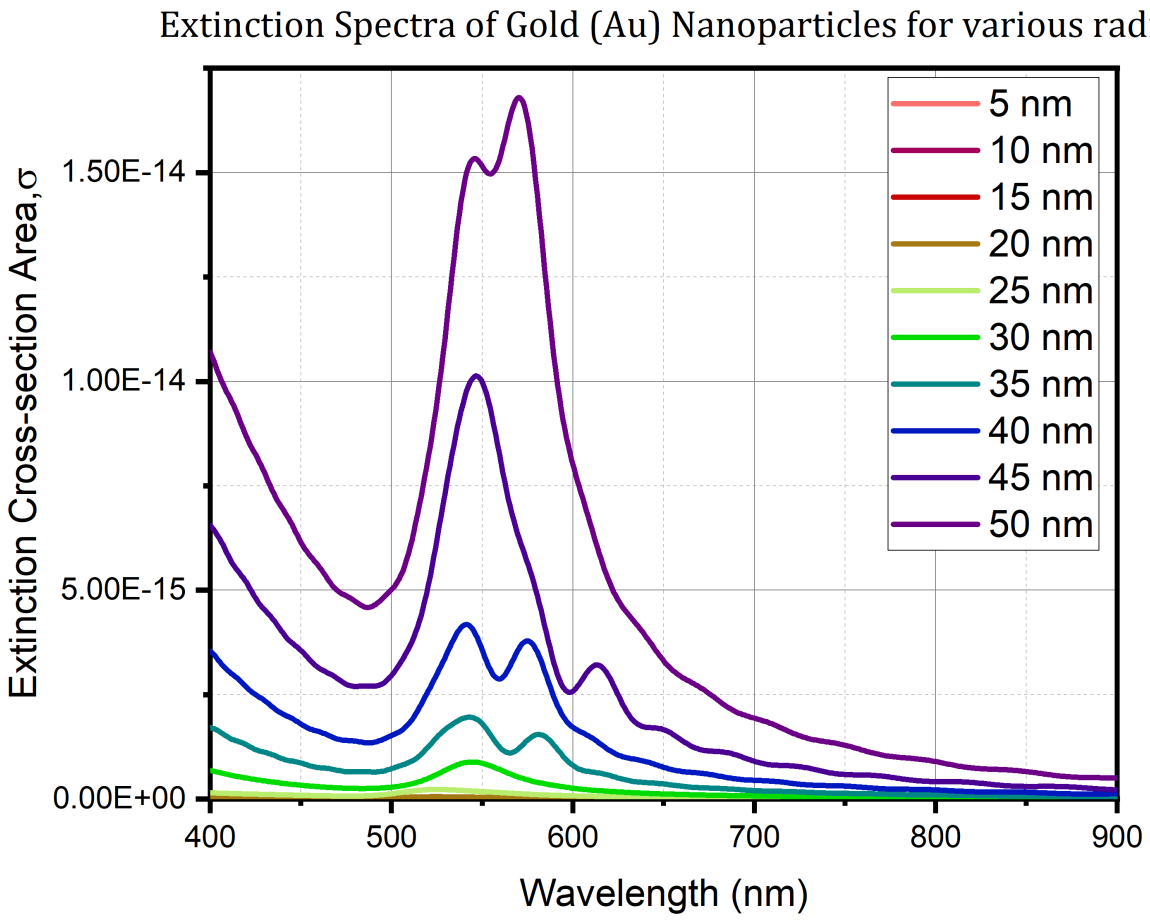

Figure 4: UV-Visible Spectra for Au nanoparticles

The Gold (Au) nanoparticle spectra has a peak near 550 nm. The Localised Surface Plasmon Resonance of gold nanoparticles accurs 550 nm, which means that they absorb green light. As a result, they show the complementary color of green, which is red. On sight, gold nanoparticles appears wine red in colour.

The UV-visible spectra of Silver Nanoparticles is shown below.

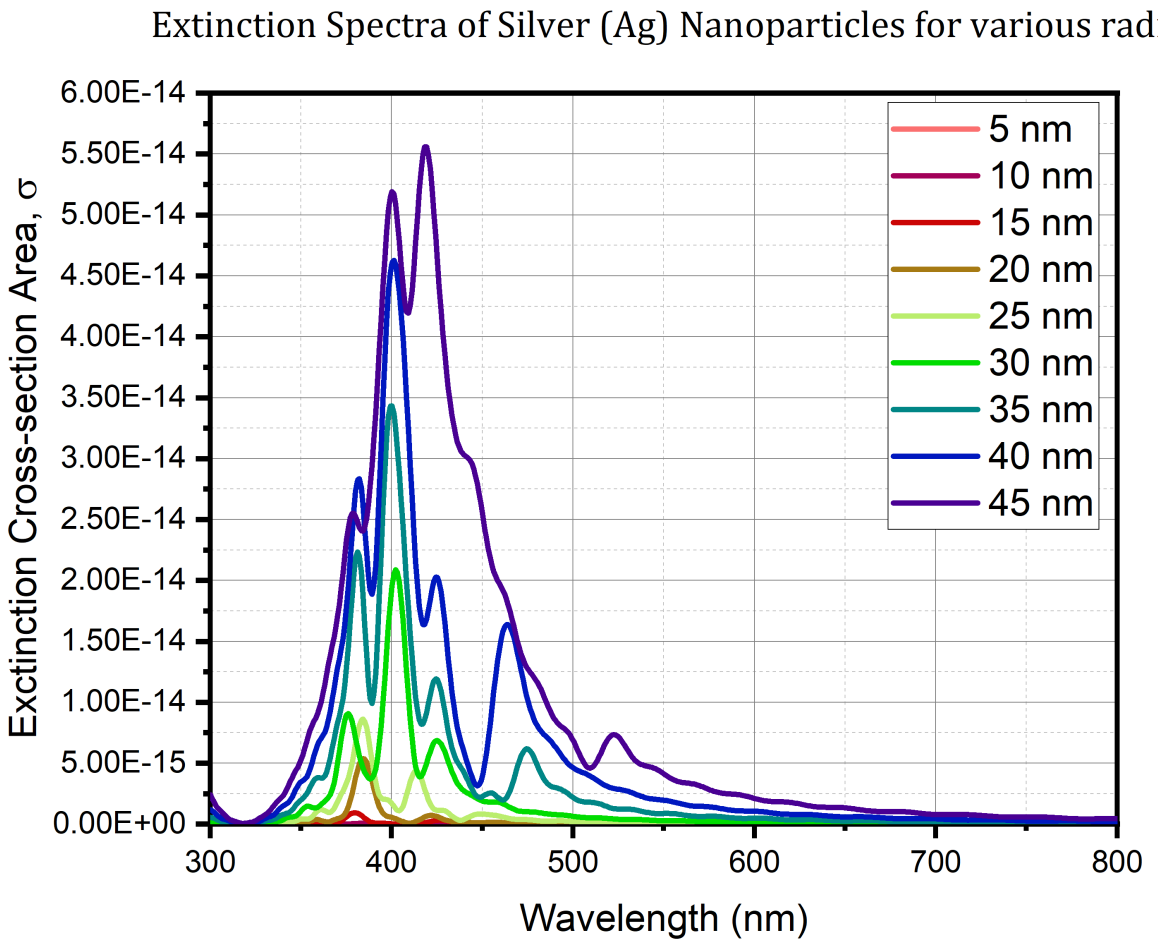

Figure 5: UV-Visible Spectra for Ag nanoparticles

The Silver (Ag) nanoparticle spectra has a peak around 400 nm. The Localised Surface Plasmon Resonance of silver nanoparticles occurs around 400 nm, which means that they absorb blue light. As a result, they appear yellow in colour.

The scattering cross-section in both cases (Fig. 4 and 5) increases with the increase in the size of the particle.

The plot of the variation of spectra peak with radii for Au nanoparticles is shown below.

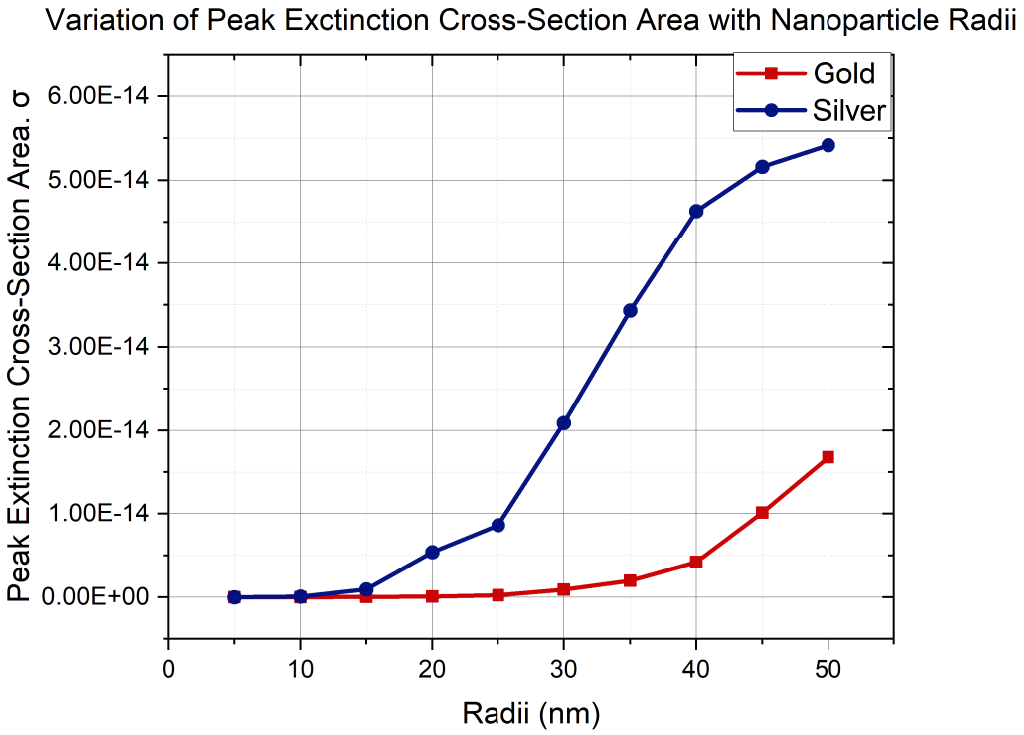

Figure 6: Change of spectra as function of particle radii

The cross-section area of Ag nanoparticles is higher than that of Au nanoparticles for all sizes, as silver scatters more light than gold.

e. What do you observe after adding the NaCl solution? Explain the extinction curves. Give a qualitative analysis by simulating in Lumerical.

Addition of NaCl solution results in the change of shape of the gold particles as they can interact and aggregate in the presence of ions. This is due to the coulombic interactions made possible by the positively and negatively charged ions. The aggregation state of gold nanoparticles has an effect on their optical properties. This can be qualitatively studied by simulating ellipsoid Au nanoparticles and observing their spectra. The higher the concentration of the NaCl solution, more is the deviation of the nanoparticle shape.

In Lumerical, ellipsoid nanoparticles are constructed with a source of polarization angle of 0 degree and their extinction spectra is plotted as shown below.

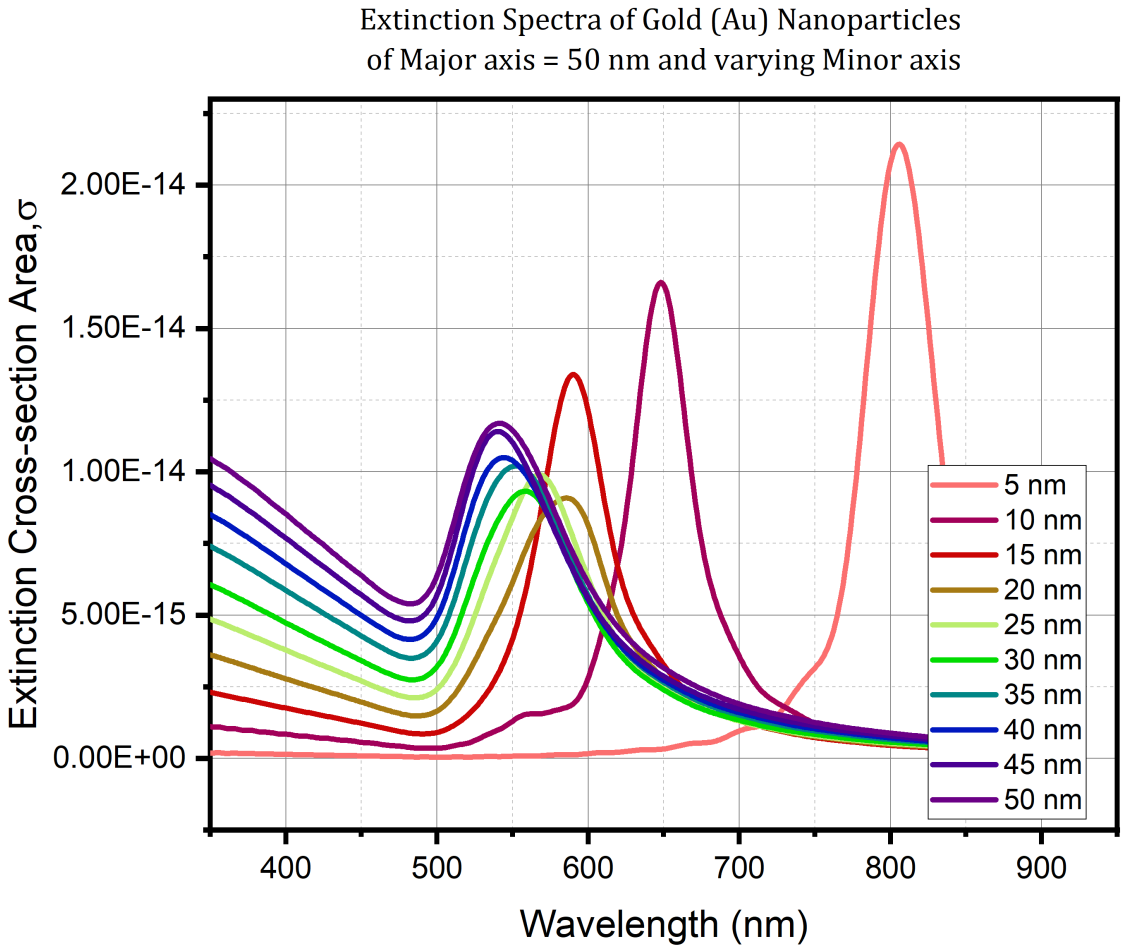

Figure 7: Extinction curves for different concentration of NaCl - ellipsoids with source polarization angle = 0°

Next, the ellipsoid nanoparticles are subjected to a source of polarization angle of 90 degrees and their extinction spectra is plotted as shown below.

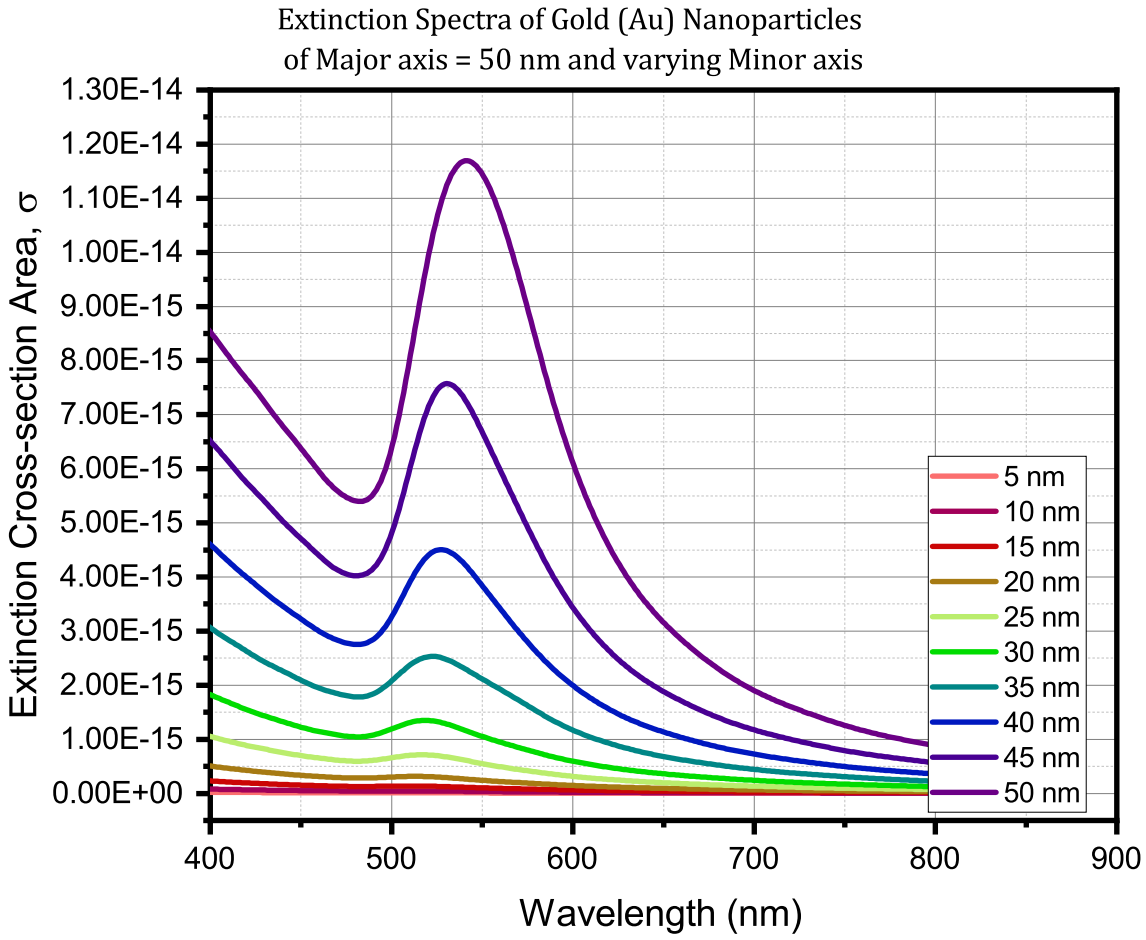

Figure 8: Extinction curves for different concentration of NaCl - ellipsoids with source polarization angle = 90°

The extinction curves obtained in polarized light are a superposition of the ones obtained in light polarized in different directions as shown in Fig. 7 and 8. The resultant extinction spectra is plotted below.

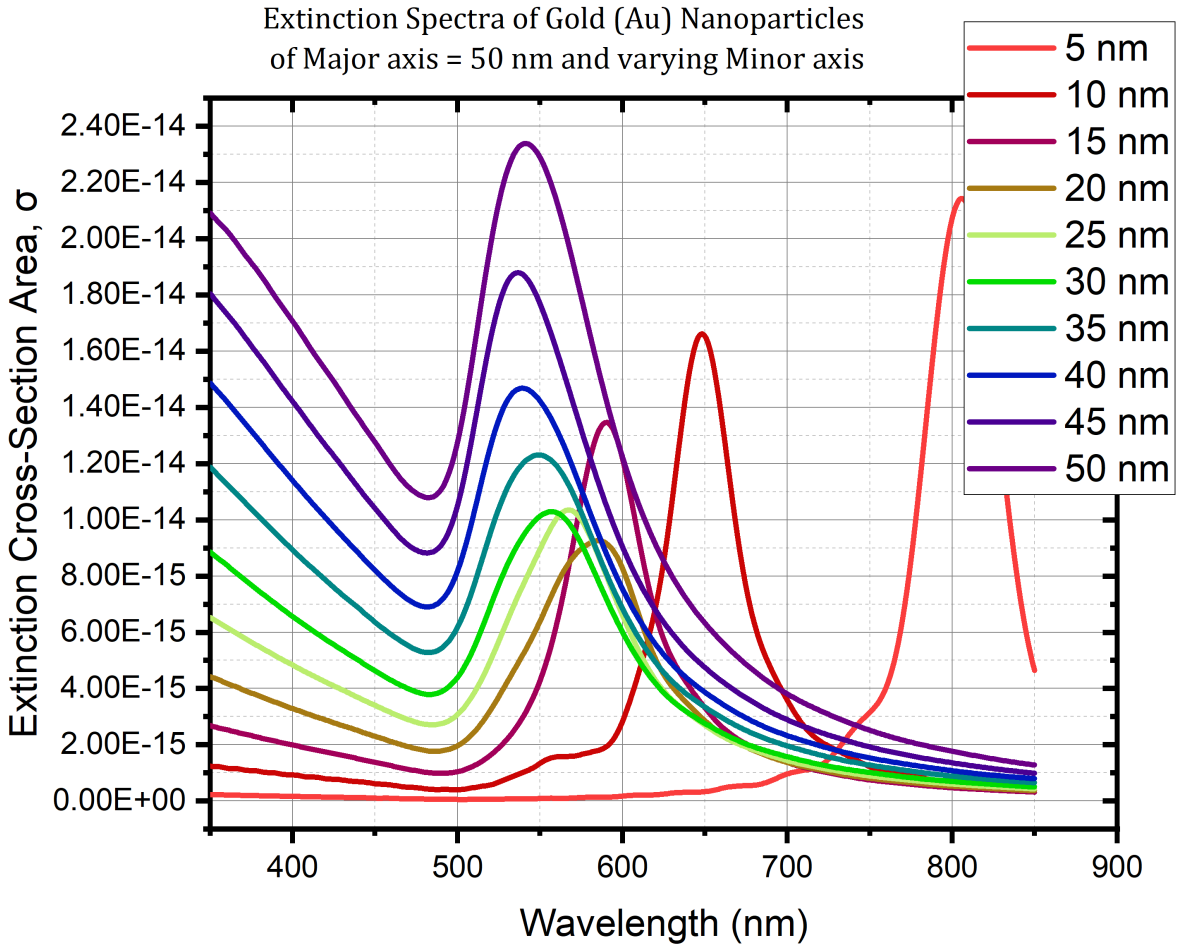

Figure 9: Total Extinction curves for different concentration of NaCl in unpolarised light

It can be seen that with an increase in the concentration of NaCl, the peak moves towards higher wavelength. In Fig. 9 the peak moves from 550 nm to ~ 650 nm. This change in spectra indicates a change in the colour of the Au nanoparticles. As the NaCl concentration increases, the nanoparticles turn from wine red to violet.

f. Using Lumerical show how the extinction properties changes as a function of surrounding refractive index for Gold, Silver and Gallium nanoparticles (particle radius 10-50 nm). Plot the sensitivity curve. Which nanoparticle system has the highest sensitivity? Explain why.

Optical properties also depend on the refractive index near the nanoparticle surface. As the refractive index near the nanoparticle surface increases, the nanoparticle extinction spectrum shifts to longer wavelengths (known as red-shifting). Practically, this means that the nanoparticle extinction peak location will shift to shorter wavelengths (blue-shift) if the particles are transferred from water (n=1.33) to air (n=1.00), or shift to longer wavelengths if the particles are transferred to oil (n=1.5).

The plot of the Gold (Au) Nanoparticle spectra for different refractive index is shown.

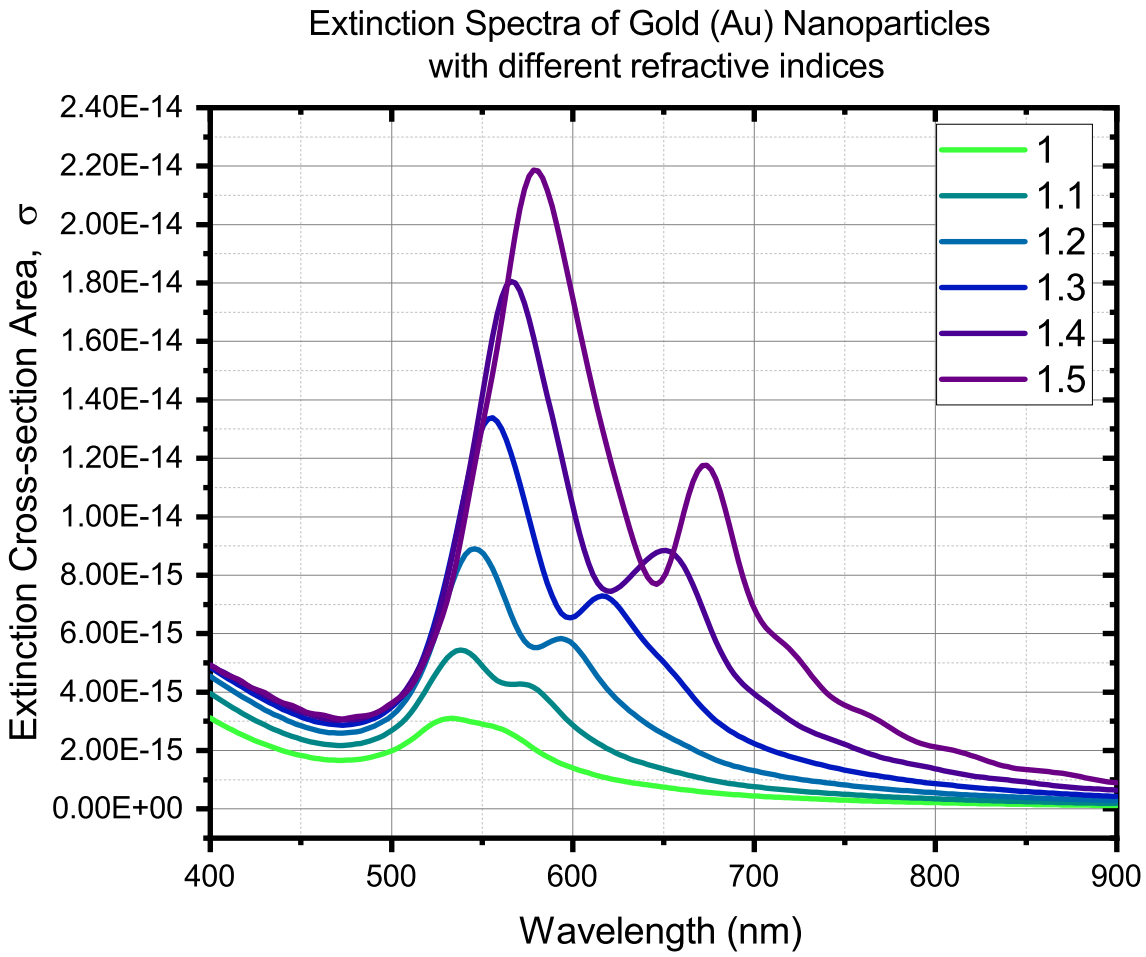

Figure 10: Gold (Au) Nanoparticle spectra for various refractive indices

The plot of the Silver (Ag) Nanoparticle spectra for different refractive index is shown.

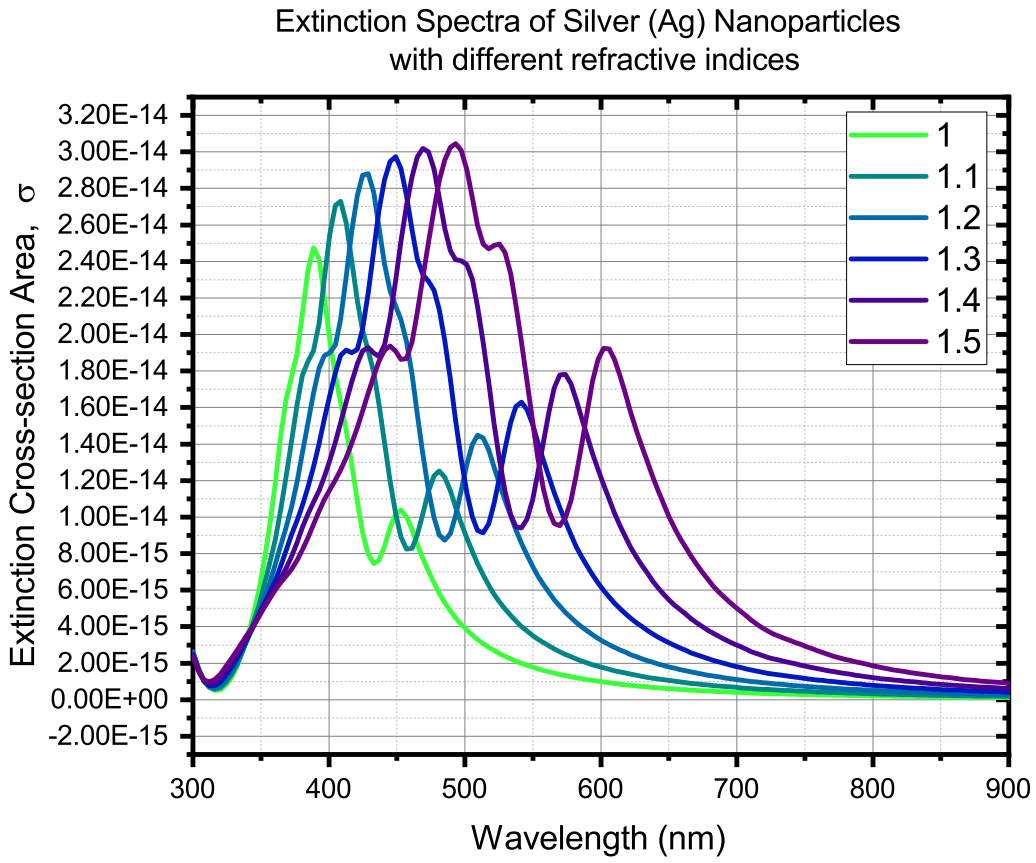

Figure 11: Silver (Ag) Nanoparticle spectra for various refractive indices

The plot of the Gallium (Ga) Nanoparticle spectra for different refractive index is shown.

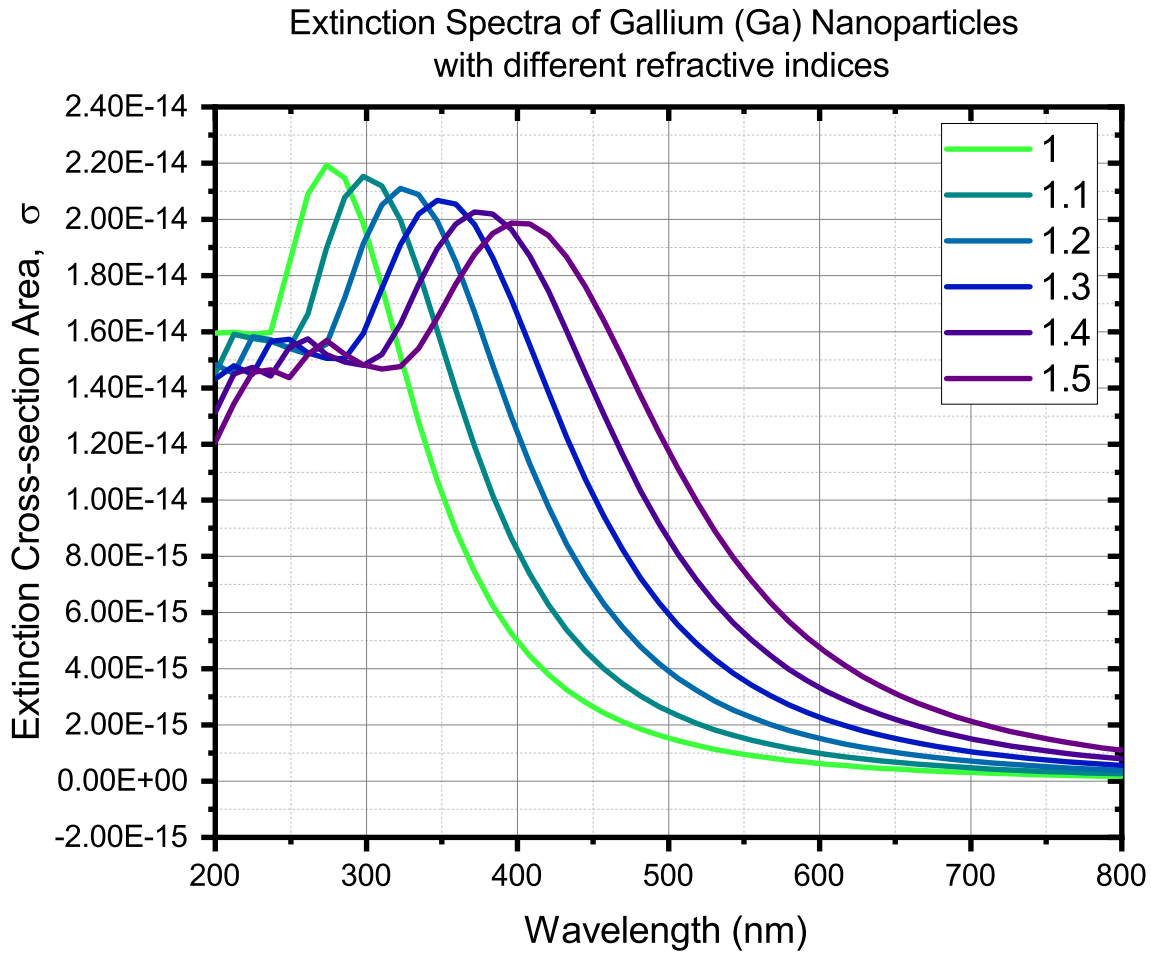

Figure 12: Gallium (Ga) Nanoparticle spectra for different refractive indices

The figures 10, 11 and 12 display the calculated extinction spectrum gold, silver and gallium nanoparticles, of radius equal to 40 nm, as the local refractive index is increased. Increasing the refractive index from 1.00 to 1.50 results in an extinction peak shift, moving the peak from the blue to the red region of the spectrum. When embedded in high index materials, the extinction cross section is substantially increased.

The sensitivity curves based on the results of the simulation are plotted below.

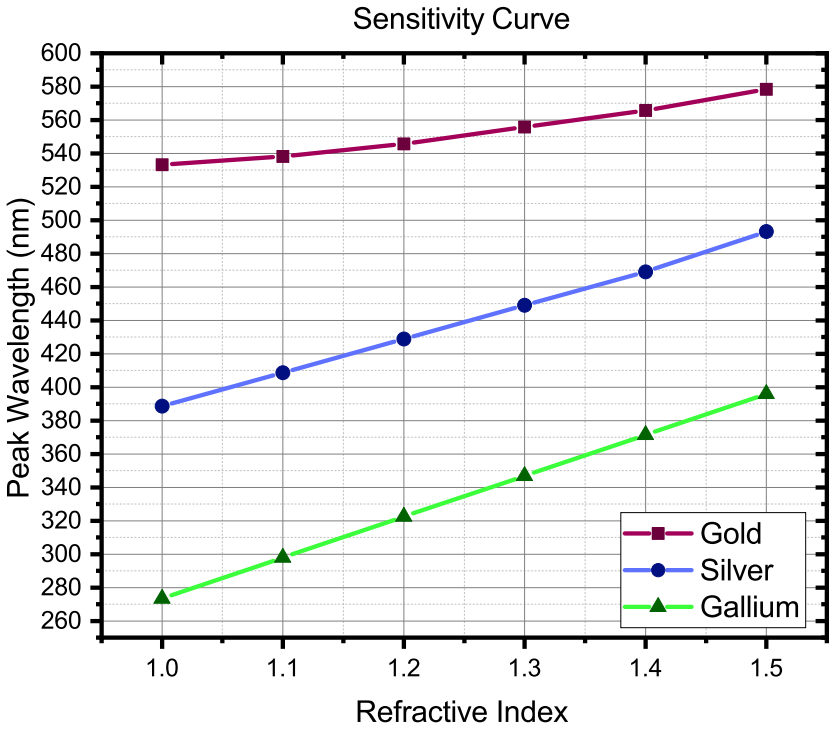

Figure 13: Peak wavelength versus Refractive index plot for Gold (Au), Silver (Ag) and Gallium (Ga) nanoparticles

The slope of the Gold (Au) curve in Fig. 13 is ~ 90 nm.
The slope of the Silver (Ag) curve in Fig. 13 is ~ 210 nm.
The slope of the Gallium (Ga) curve in Fig. 13 is ~ 245 nm.

It can be inferred from these values that Gallium has the highest sensitivity and gold has the lowest. The sensitivity of the material depends on the difference between the refractive index of the nanoparticle and of the surrounding. Since Gallium has the highest different it varies the most, followed by silver and with gold at last. It is also due to losses in the nanoparticles arising from the imaginary part of the dielectric constant of the materials.

It can also be observed that the curves broaden with an increase in the surrounding refractive index. For a narrow spectra, surrounding refractive index should be low.

INDIAN INSTITUTE OF SCIENCE

DEPARTMENT OF INSTRUMENTATION AND APPLIED PHYSICS

IN252 - OPTICS: MATERIALS AND DEVICES

Assignment 7

Chaitali Shah
(SR No: 01-02-04-10-51-21-1-19786)

Date: November 29, 2023

Near unity reflecting mirrors using dielectric metasurface

Metasurface are artificial 2D planar structures engineered at scales that are smaller than their functional wavelengths. They can be designed to exhibit many unprecedented electromagnetic phenomena such as negative refraction, near zero refraction, hyperbolicity, and optical chirality. However, metals have relatively high absorption loss at optical frequencies, which limits the applications of the metal-based metamaterials in photonics.

1. If you are given three materials TiO2, Si and Se which one will you use to achieve perfect reflection in the visible and why?

The relation between energy and wavelength is given using

$$\lambda(\mu m) = \frac{1.24(\mu m\ eV)}{E(eV)} \tag{1}$$

The band gap of $TiO_2 \sim 3.2$ eV.
The corresponding wavelength is found (using Eq. 1), to be ~ 387 nm.
The band gap of Si ~ 1.12 eV.
The corresponding wavelength is found (using Eq. 1), to be ~ 1107 nm.
The band gap of Se ~ 1.95 eV.
The corresponding wavelength is found (using Eq. 1, to be ~ 635 nm.
Visible light has wavelength ranging from 400 nm to 750 nm.

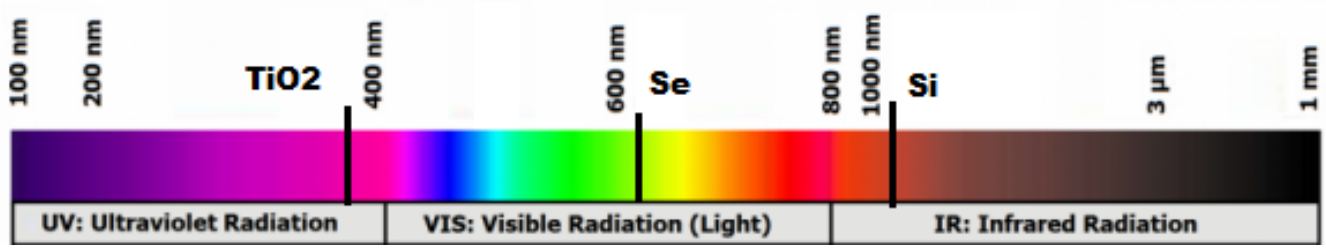

Figure 1: Electromagnetic Spectra with wavelengths corresponding to band gaps of TiO_2, Se and Si

The material absorbs photons that have energies that are higher than to equal to the band gap energy. The photons of lower energies are reflected. In terms of wavelength, the material absorbs light of wavelength lower than that corresponding to the band gap and reflects all the light above that wavelength.

So, for perfect reflection in the visible range the material has to be such that its wavelength is less than 400 nm. Among the choices given, only TiO_2, with band gap wavelength ~ 387 nm, satisfies this criteria.

Therefore, we can use TiO_2 to achieve perfect reflection in the visible range.

2. Perform FDTD simulation on a monolayer of TiO2 spheres embedded in air. Change the particle diameter and array period to achieve near unity reflection in R G B region.

A unit cell of the monolayer of TiO2 is generated in the simulation using a sphere with its material as TiO2 as shown in Fig. 2.

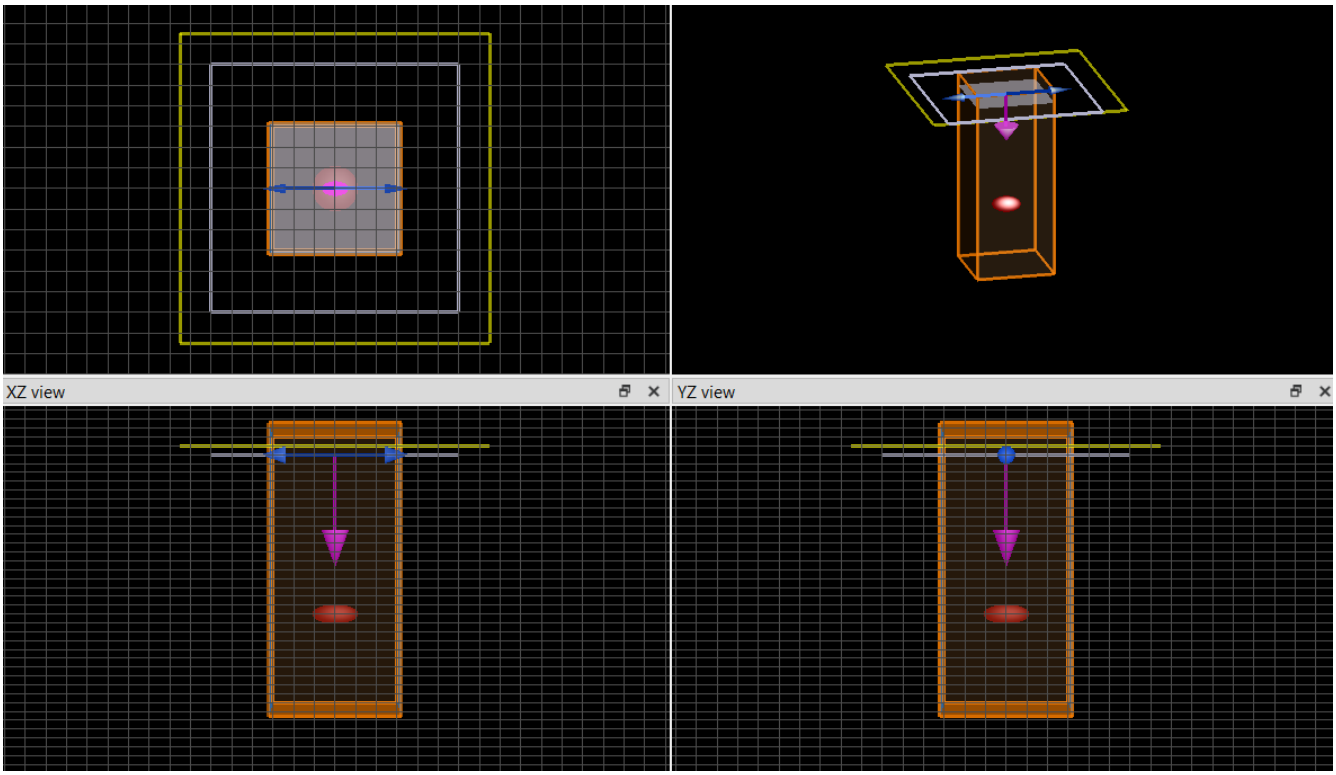

Figure 2: FDTD simulation of monolayer of TiO2 spheres embedded in air

The simulations are carried for various sizes of the FDTD simulator and mesh (400 nm, 500 nm, 600 nm and 700 nm). The size of the FDTD simulator and mesh correspond to the periodicity of the lattice as the boundary conditions of the FDTD simulator in the XZ and YZ planes is Periodic. The boundary condition for the XY planes of the simulation region is PML (Perfectly Matched Layer).

In each run of the simulation, the radius of the nanosphere is swept for 5 different values to discern the value at which the reflectivity is nearest to unity and the peak is the narrowest at a particular wavelength. The results obtained are plotted in Fig. 3, 4, 5 and 6.

The Reflectivity versus Wavelength plots for a periodicity of 700 nm is shown in Fig. 3.

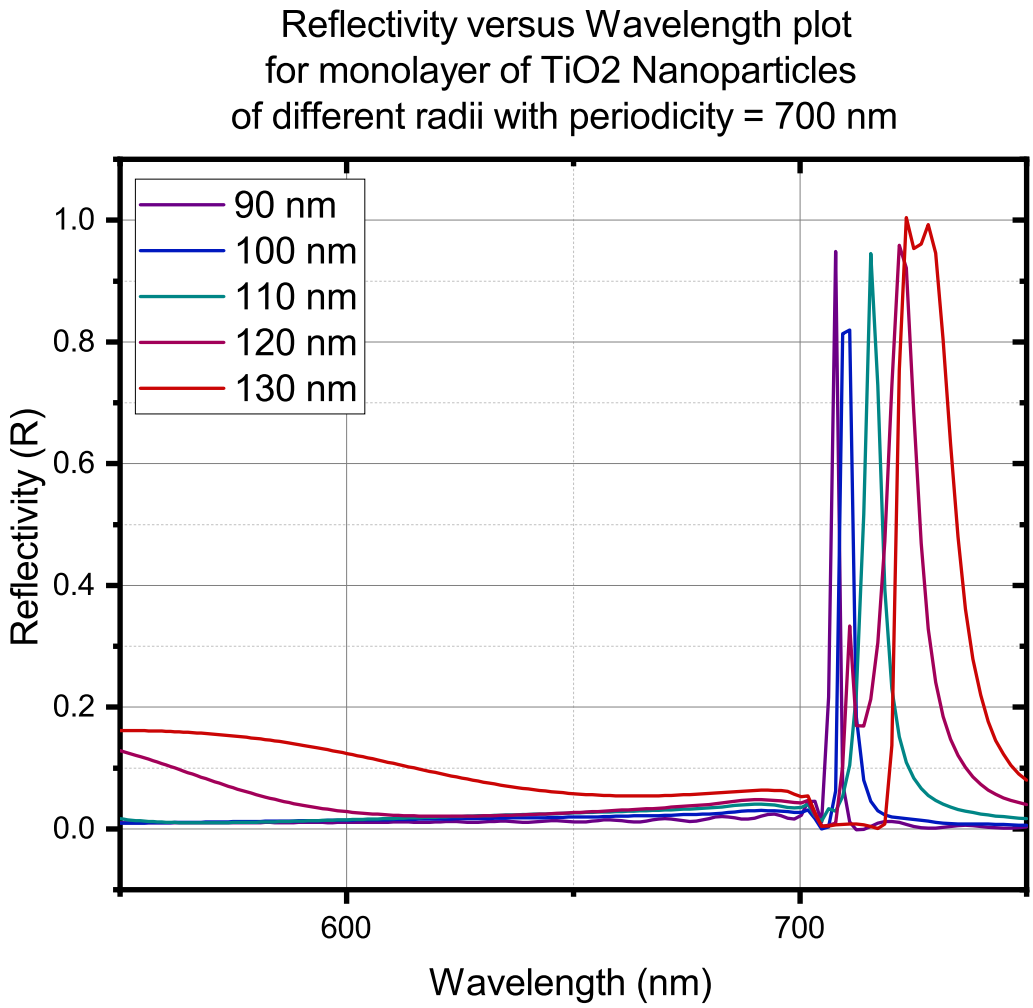

Figure 3: Reflectivity versus Wavelength for Periodicity = 700 nm. Particle radii is varied from 90 nm to 130 nm

It is observed that the peak in reflectivity for a particle radius of 90 nm is obtained at a wavelength of 710 nm. With an increase in particles size, the wavelength peaks shift rightward. Also the value of reflectivity increases with the particle size. The width (FWHM) of the peak also increases and there are multiple peaks as seen in the case of particle radius of 130 nm.

The optimum radius is 120 nm where the reflectivity has a value 0.959 while retaining a single peak. As the reflectivity is at 720 nm, the material reflect red light.

The Reflectivity versus Wavelength plots for a periodicity of 600 nm is shown in Fig. 4.

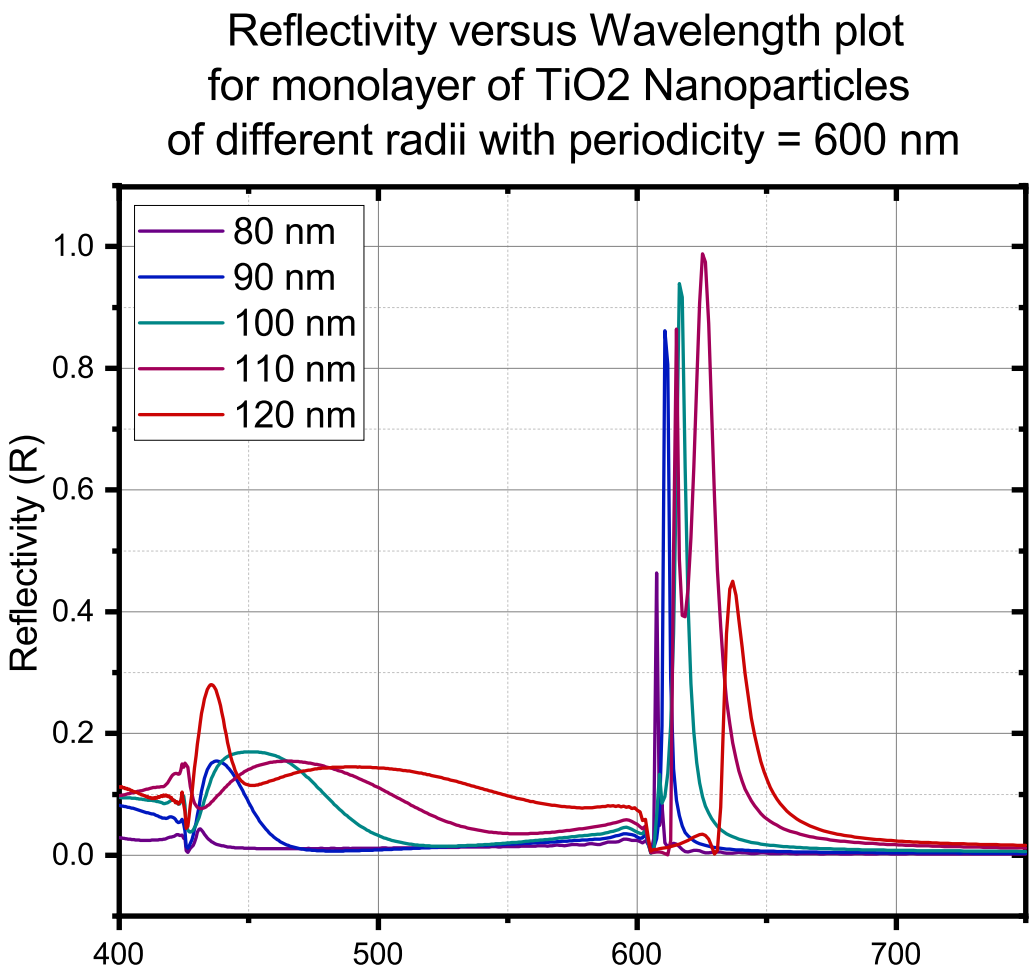

Figure 4: Reflectivity versus Wavelength for Periodicity = 600 nm

It is observed that the peak in reflectivity for a particle radius of 80 nm is obtained at a wavelength of 610 nm. The reflectivity is very low for this size but increases with an increase in the particle size. The rightward shift of peak With an increase in particles size is also observed.

The optimum radius is 110 nm where the reflectivity has a value 0.987 while retaining a single resonance peak. The peak is at wavelength 625 nm and hence it also reflect red light.

The Reflectivity versus Wavelength plots for a periodicity of 500 nm is shown in Fig. 5.

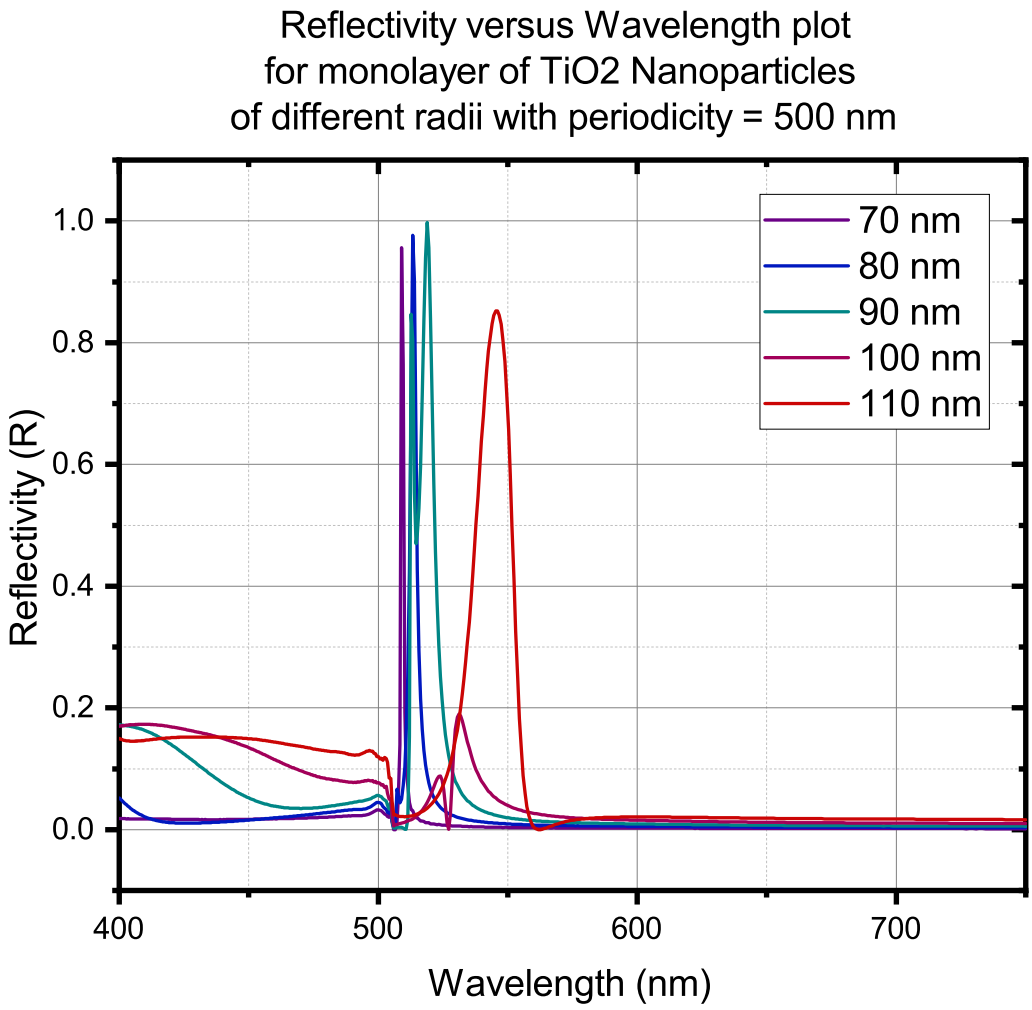

Figure 5: Reflectivity versus Wavelength for Periodicity = 500 nm

It is observed that the peak in reflectivity for a particle radius of 70 nm is obtained at a wavelength of 510 nm. The reflectivity is 0.955 at this size. The peak is sharp but becomes wider with an increase in particle size.

The optimum radius is 90 nm where the reflectivity has a value 0.997 while retaining a single peak. As the reflectivity is at 520 nm, the material reflect green light.

The Reflectivity versus Wavelength plots for a periodicity of 400 nm is shown in Fig. 6.

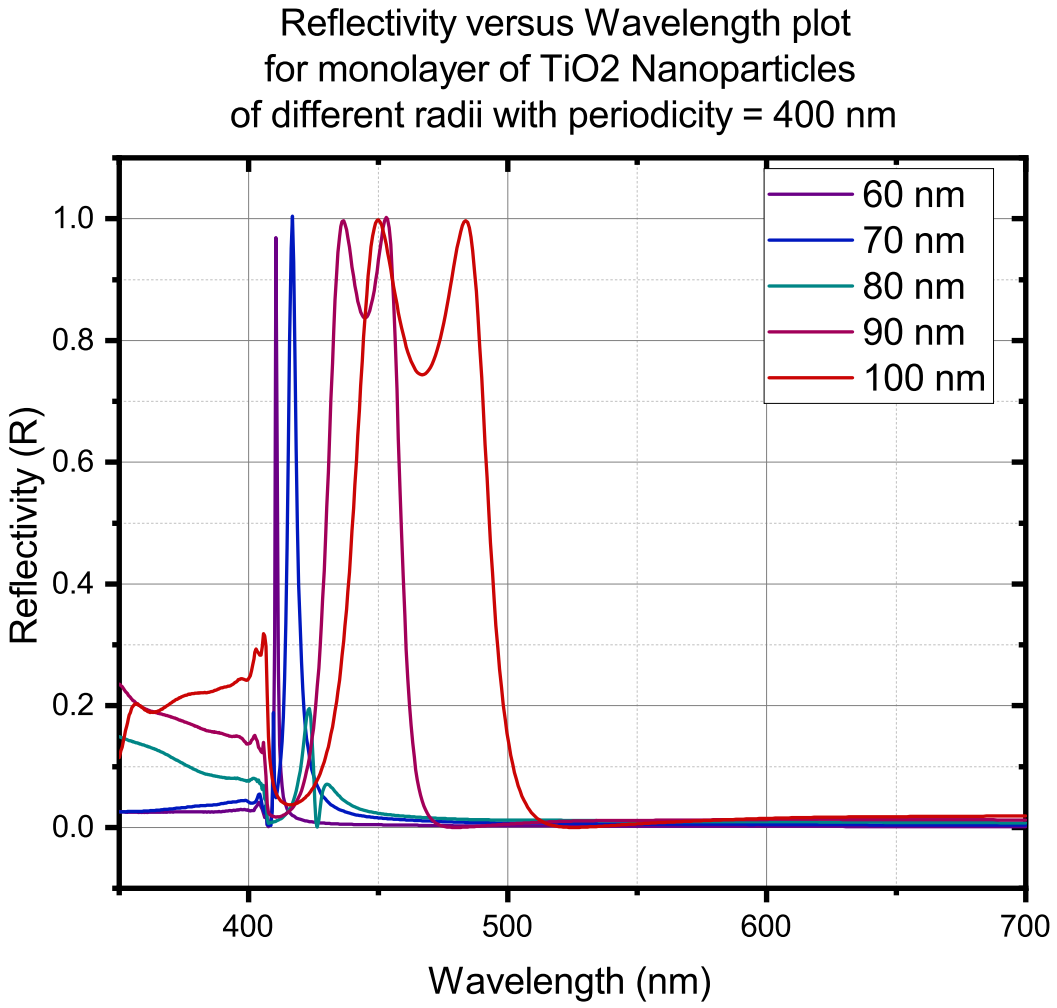

Figure 6: Reflectivity versus Wavelength for Periodicity = 400 nm

The peak in reflectivity for a particle radius of 60 nm is obtained at a wavelength of 410 nm. The reflectivity is 0.968 at this size. The peak is sharp but becomes wider with an increase in particle size. Eventually there is a formation of two peaks for higher sizes.

The optimum radius is 70 nm where the reflectivity is almost unity. As the reflectivity is at 416 nm, the material reflect blue light.

3. How will you modify your design when you have a glass substrate.

A glass substrate is added with the nanosphere embedded in it as shown in Fig. 7. This is a reasonable model for monolayers of TiO2 nanospheres that can be fabricated by lithography.

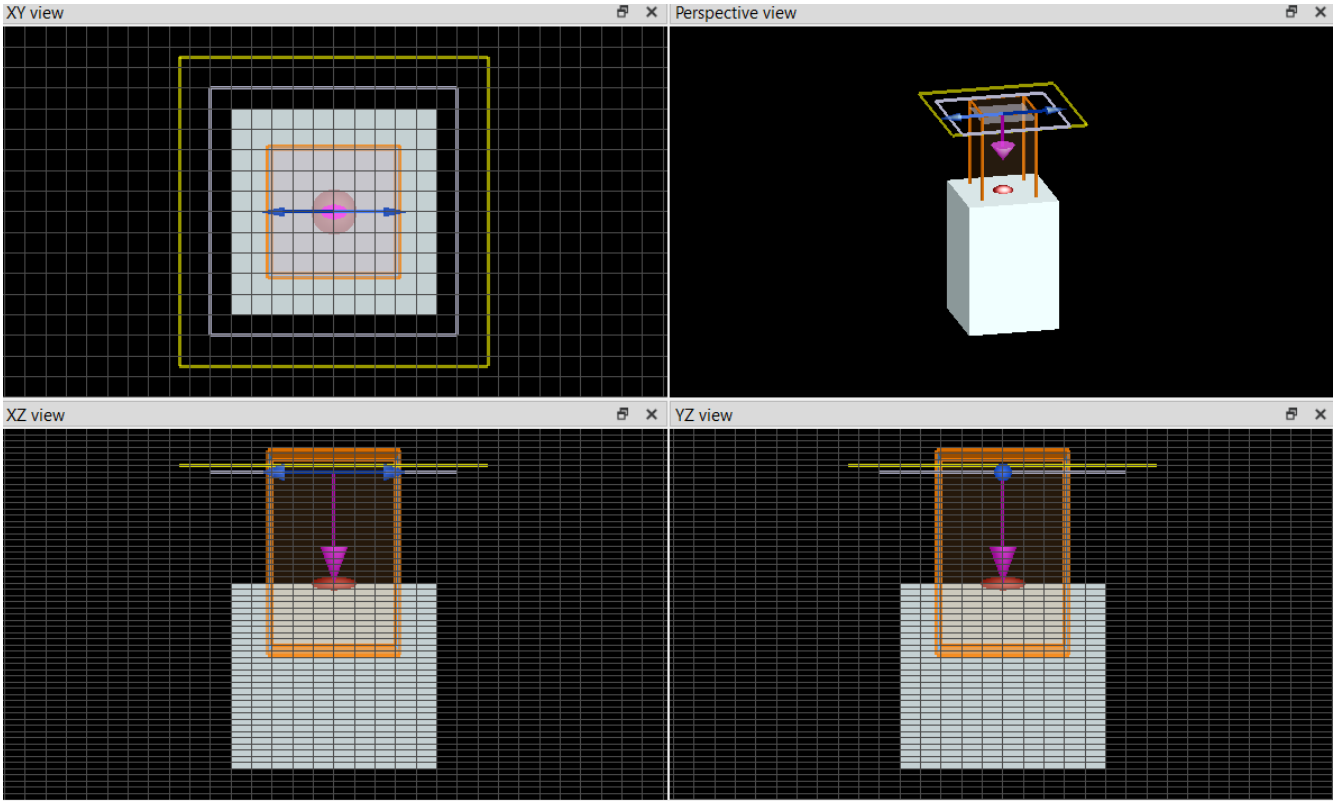

Figure 7: FDTD simulation of monolayer of TiO2 spheres embedded in glass substrate

The simulations are carried for various sizes (500 nm and 600 nm) of the FDTD simulator and mesh to give results for near unity reflectivity in the R G B region. The size of the FDTD simulator and mesh correspond to the periodicity of the lattice.

In each run of the simulation, the radius of the nanosphere is swept for 5 different values to discern the value at which the reflectivity is nearest to unity and the peak is the narrowest at a particular wavelength. The results obtained are plotted in Fig. 8 and, 9.

The Reflectivity versus Wavelength plots for a periodicity of 600 nm is shown in Fig. 8.

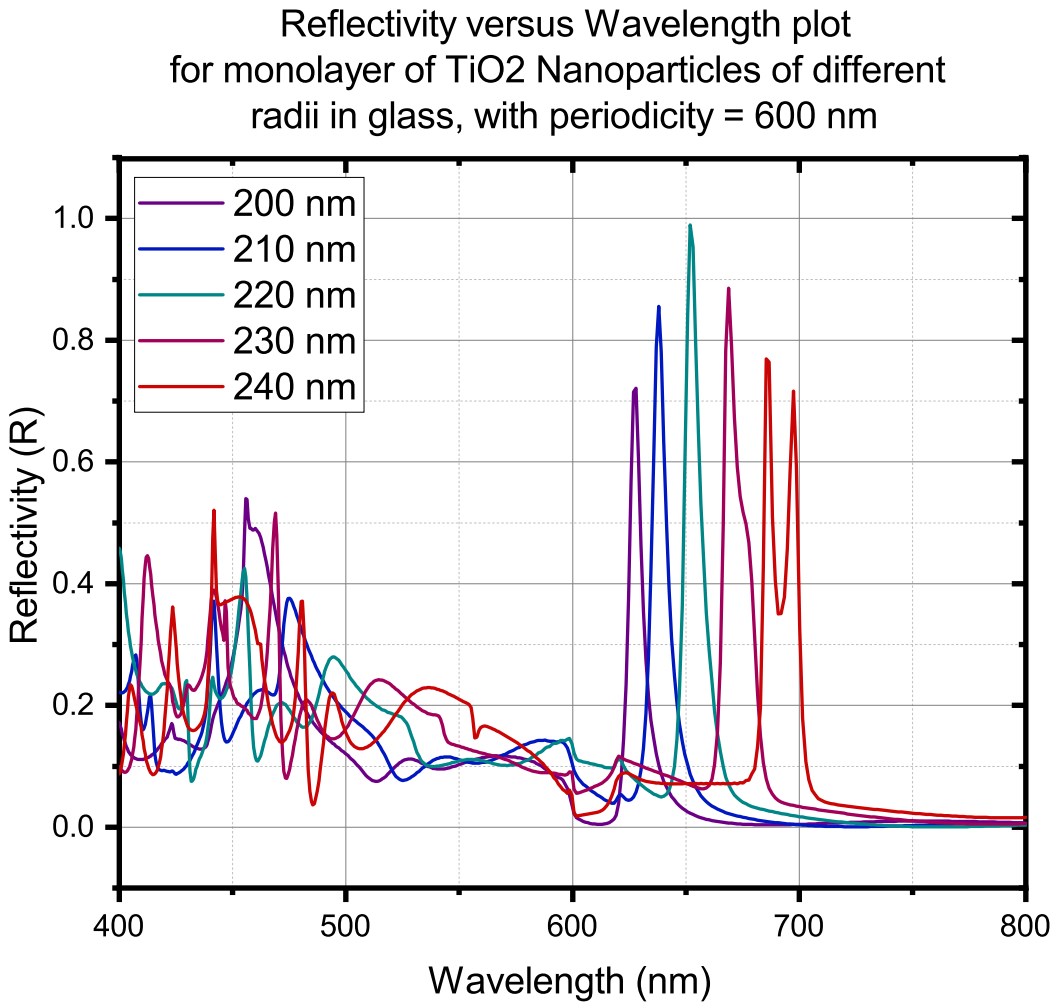

Figure 8: Reflectivity versus Wavelength for Periodicity = 600 nm

It is seen that there a sharper resonance in clear from the comparison from Fig. 4 and 8 that the peaks in reflectivity are narrower when the substrate is glass. For a particle radius of 200 nm the peak is obtained at a wavelength of 620 nm. The reflectivity is very low for this size but increases with an increase in the particle size. The rightward shift of peak with an increase in particles size is also observed.

The optimum radius is 110 nm where the reflectivity has a value 0.987 at a wavelength of 650 nm. This reflects red light. It is also evident that as the glass has a higher refractive index than air the particle size for unity reflectivity also needs to be higher.

The Reflectivity versus Wavelength plots for a periodicity of 500 nm is shown in Fig. 9.

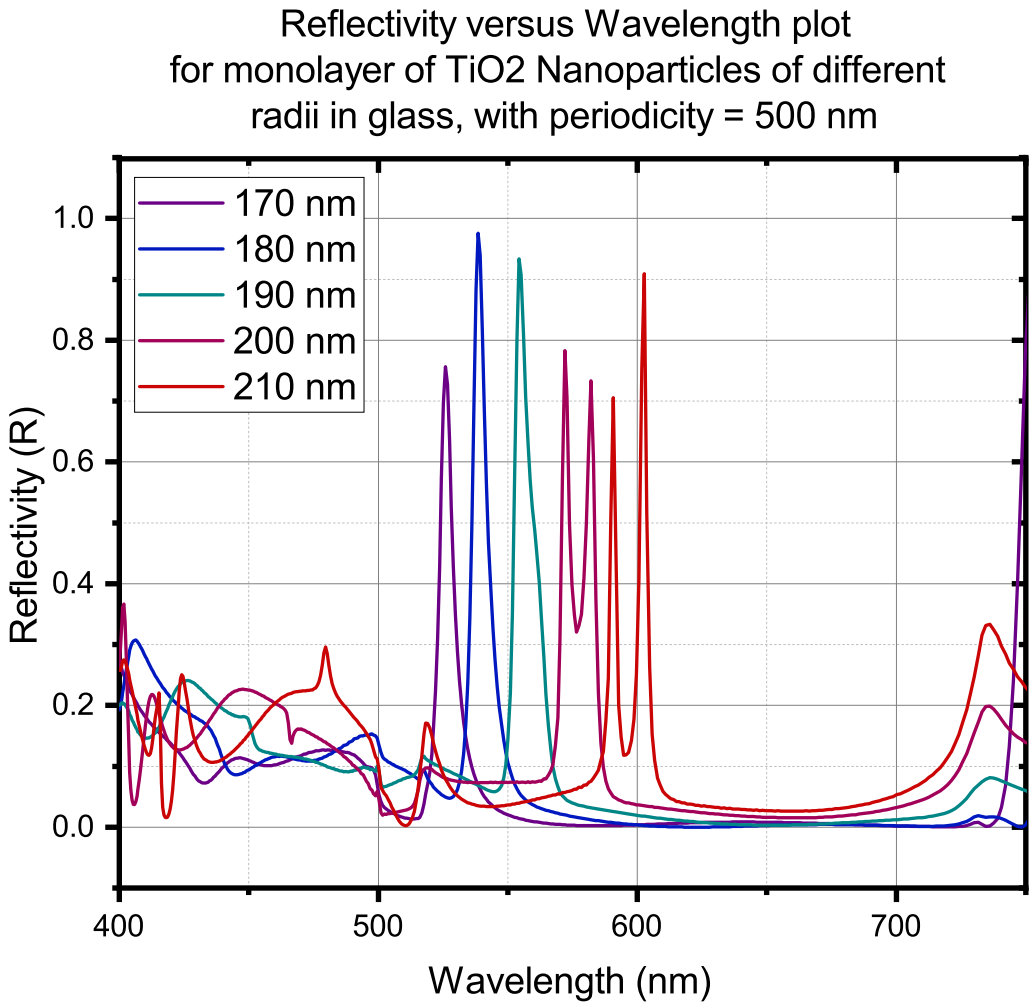

Figure 9: Reflectivity versus Wavelength for Periodicity = 500 nm

A sharper resonance is obtained in Fig. 9 as compared to 5 as glass has a higher refractive index than air. It is observed that the peak in reflectivity for a particle radius of 170 nm is obtained at a wavelength of 520 nm. The reflectivity increases with increase in particle size initially.

The optimum radius is 180 nm where the reflectivity has a value 0.975. As the reflectivity is at 538 nm, the material reflect green light. For larger values of particle radius, there is an emergence of multiple peaks. It should also be noted that there are peaks forming beyond the visible range (> 750 nm).

For lower periodicities, there are two reflectivity peaks in the visible range (red and blue light). As the periodicity decreases further, the peaks occur for wavelength below the visible region.

4. Comment on the cause of reflectivity.
The TiO2 nanoparticles arranged in an ordered array scatter light to produce diffracted waves. If one of the diffracted waves then propagates in the plane of the array, it may couple the localized plasmon resonances associated with individual nanoparticles together, leading to the narrowing of plasmon resonances in the nanometer range. It is this **plasmonic surface lattice resonance** that cause the reflectivity. These resonances emerge from the enhanced radiative coupling of localized Mie resonances in the individual nanoparticles. Such resonance occur due to both spatial and temporal matching of the waves.The resonance of the propagating via the gap between the nanoparticles and not due to formation of dipoles.

5. For applications in notch filters the FWHM should be as narrow as possible. Suggest few ways to tune the FWHM.

- The FWHM was narrower in the case of glass as compared to that of air. This shows that adding a substrate with a higher refractive index can improve the sharpness of the peak.
- The size of nanoparticles also has to be optimised as FWHM decreases with the decrease in the size of the particles. So the size has to be chosen such that FWHM is low, while retaining a good reflectivity.
- The shape of the particles is also an important factor for the reflectivity spectrum. The simulation uses spheres but realistically particles can be like droplets or pyramidal (as in the case of dewetting). In practice, cylindrical nanoparticles give excellent results as there is resonance along two axes, leading to a sharper resonance and lower FWHM.

6. Near unity reflection can also be achieved with DBRs (last assignment). Which one you will prefer in terms of fabrication.
Fabrication of DBR might seem easier at the first glance but one also has to consider the number of layers required. If many layers are required to obtain near unity reflection, it caused strain in the DBR and the sample might break. The materials have to be lattice matched and should have less layers for the DBR to be convenient from the fabrication point of view. Hence, nanoparticle arrays are better to fabricate using lithography. It also allows for a lot of flexibility in terms of the design of the material. Cylindrical (micropillar) particle arrays are especially preferrable in terms of fabrication.